JOURNAL OF QUATERNARY SCIENCE (2025) **40**(6) 1070–1096 ISSN 0267-8179. DOI: 10.1002/jqs.3729

JQS Journal of Quaternary Science QRA Quaternary Research Association

# Vegetation and environmental dynamics in the central part of the Kola Peninsula during the past 13.3 ka as reflected by ancient plant DNA on sediments from Lake Imandra

**ANASTASIA POLIAKOVA,[1,2]* MATTHIAS LENZ,[3] MARTIN MELLES,[3] GRIGORY FEDOROV,[4,5] MARIE K. F. MERKEL[1] and INGER G. ALSOS[1]**

[1]Tromsø University Museum, UiT—The Arctic University of Norway, Tromsø, Norway
[2]Institute for Chemistry, University of Hamburg, Hamburg, Germany
[3]Institute of Geology and Mineralogy, University of Cologne, Cologne, Germany
[4]St. Petersburg State University, St. Petersburg, Russia
[5]Arctic and Antarctic Research Institute, St. Petersburg, Russia

Received 13 March 2024; Revised 12 May 2025; Accepted 28 May 2025

ABSTRACT: The first high-resolution reconstruction of the vegetation and environmental changes during the last ca 13 300 cal a BP in the central part of the Kola Peninsula (NW Russia) was reconstructed based on sedimentary ancient DNA (*sed*aDNA) metabarcoding on sediment core Co1410 from Lake Imandra. In total, 204 taxa known from modern flora are identified. The resulting sequences were assigned to vascular plants (87%), bryophytes (12%), and algae (1%). About half (111 taxa, 49%) are identified at the species level. They belong to 150 genera and 86 families. So far, this is the most diverse and taxonomically detailed palaeoflora described for the Late Pleistocene–Holocene of the Kola Peninsula and North-European Russia. *Sed*aDNA studies suggest that the vegetation cover in the region developed from (1) plant colonisation of the study area after the glacier retreated during the Allerød warming at ca 13 300–13 000 a BP to (2) Younger Dryas cold period with re-entering of the glaciers in the catchment of the Grater (Bolshaya) Imandra and establishing of the steppe–tundra communities. (3) Warming and increasing in vegetation diversity during the Early Holocene, with the formation of the birch forests by the end of this time zone. (4) Mid-Holocene temperature maximum is correlated with the highest regional plant diversity and a pronounced role of the thermophilic taxa, that is, *Lonicera* species, *Prunus padus, Populus tremula, Sorbus sp./Cotoneaster* sp. The highest so far revealed regional diversity of the higher spore plants (10) and aquatic plants (23) is evidenced. Mixed deciduous and coniferous forests were established in the research area during this period, and a drop in plant diversity occurred afterwards. (5) During the Late Holocene, modern communities are formed with a slight increase in biodiversity because of increasing input from cultural plants and weeds. Human impact is clearly diagnosed after 250 a BP, indicated by the presence of *Ribes* sp., *Hypericum* sp., and *Mentha arvensis* as well as eutrophic weeds, that is, *Trifolium* sp. and *Urtica dioica*. In addition, this study revealed the past dynamics of some plants rare for the Murmansk region, namely *Pteridium aquilinum,* with its maximum of occurrence at ca 11 000–8000 cal a BP and a strong decrease thereafter, and *Nuphar* sp./*Nymphaea* sp. occurring regularly since ca 7700 cal a BP and eliminating from the record after ca 3500 cal a BP.
© 2025 The Authors *Journal of Quaternary Science* Published by John Wiley & Sons Ltd.

KEYWORDS: Allerød warming; Lake Imandra; palaeoenvironmental reconstruction; sediment ancient DNA; vegetation history

## Introduction

In general, the geological and palaeobotanical history of the Kola Peninsula (NW Russia) from the Last Glacial Maximum to the present is well-documented. Korsakova (2020) provides a comprehensive summary of the Upper Pleistocene and Holocene stratigraphy, incorporating lithological, geochronological, and palaeoenvironmental proxies (i.e., pollen and spores, diatoms, foraminifera, and mollusks) and correlating stratigraphic subdivisions of the regional Quaternary system (Zhamoida et al., 2006; Zastrozhnov et al., 2014) and their international analogues as used in the International Stratigraphic Chart (Cohen and Gibbard, 2011; Head and Gibbard, 2015) and in the Stratigraphic Guide of the International Commission on Stratigraphy, 2013 (https://stratigraphy.org/).

As Solovieva and Jones (2002) indicate, the earliest palaeoecological and palaeolimnological studies in the Kola Peninsula based on pollen studies were apparently performed by Aario (1943), who worked in Petsamo (at present: Pechenga, Печенга in Russian) using data from the Arctic Ocean coast and describing major changes in the Northern to Central European forests and climate history during the postglacial period. Subsequent research also focused on pollen and diatom analyses to capture major postglacial vegetation and climate dynamics (Sorsa, 1965; Davydova and Servant-Vildary, 1996; Elina et al., 1995). While these studies offered insights into regional environmental history, they often lacked detailed resolution and reliable dating. Further palaeoecological and palaeogeographical research available from the mid-80s focuses on the glacial history of the greater regions

*Correspondence: A. Poliakova, as above.

E-mail: anastasia.poliakova@uni-hamburg.de

© 2025 The Authors *Journal of Quaternary Science* Published by John Wiley & Sons Ltd.
This is an open access article under the terms of the Creative Commons Attribution License, which permits use, distribution and reproduction in any medium, provided the original work is properly cited.

like Scandinavia, Fennoscandia, the Barents Sea, and Northern Eurasia. These studies described ice sheet dynamics and the related large-scale environmental changes (e.g., Lundqvist, 1986; Elverhøi et al., 1993; Lundqvist and Saarnisto, 1995; Kleman et al., 1997; Kleman and Hättestrand, 1999; Boulton, 2001; Svendsen et al., 2004; Kleman and Glasser, 2007; Hughes et al., 2016; Stroeven et al., 2016; Patton et al., 2017).

Significant advances in understanding the regional palaeoecological patterns came with well-dated vegetation and climate records. Kremenetski et al. (1997) suggested ice-free areas in southeast Kola Peninsula around ca 11 000–10 000 a BP, with forest-tundra establishing by ca 10 000 a BP and birch forests peaking between ca 9000 and 8000 a BP. The expansions of *Pinus sylvestris* and *Picea obovata* were documented, highlighting climatic influences and migration patterns of the trees (MacDonald et al., 2000; Seppä and Birks, 2001). These findings correlate with Northern Fennoscandia and broader Arctic trends (Snyder et al., 2000).

The recent palynological studies in the central Kola Peninsula from the lake Kamenistoe (Krikunova et al., 2022) suggested ice-free conditions much earlier than the one discussed above, that is, already at ca 13 000 a BP. Furthermore, the authors argue that "the Lateglacial spread of arboreal taxa as well as the spread of pine and spruce in the Holocene did not follow a zonal expansion," but originated from the scattered pioneer populations within the study area. The latter hypothesis supports an earlier scenario for the regional vegetation development offered by Velichko et al. (2017 and Fig. 3 within) in the form of the regional palaeovegetation maps depicting open woodlands with birch and pine trees in association with herbaceous and dwarf shrub-moss tundra in the central part of the Kola Peninsula.

As demonstrated, the past vegetation of the Arctic and Northern Europe (e.g., Bjune et al., 2005; Anisimov and Moskalenko, 2006; Seppä et al., 2008; Bernardova and Košnar, 2012; Poliakova et al., 2024) including those in Murmansk Region and the Kola Peninsula (Nikonov and Vostrukhina, 1964; Grave et al., 1969; Snyder et al., 2000; Korsakova, Kolka, Semenova, 2016a; Korsakova, Kolka, Tolstobrova, et al., 2016b; Krikunova et al., 2022) is studied largely by using pollen and spore analysis which is a powerful method if applied on the regional scale, although it allows identification mainly at the higher taxonomic levels, that is, family and genera. To be applied at the species level, it requires strong knowledge of pollen morphology and can be limited by the levels of pollen preservation. Some pollen and spores, when buried in sediments, tend to lose diagnostic features (e.g., pollen grains of Rosaceae, some fern spores, and bryospores). Additionally, long-distance pollen component and details on the wind directions have to be considered as the Arctic is known for diverse pollen spectra with a high proportion of the extra-regional pollen (Campbell et al., 1999; Rousseau et al., 2003; Poliakova et al., 2024) as well as for reduced pollen and spore production due to specific environmental conditions. Limited pollen accumulation rates can restrict the application of the pollen-based environment reconstructions in the Arctic and sub-Arctic conditions.

Analysis of the plant sedimentary ancient DNA (*sed*aDNA) can help resolve problems of taxonomical resolution and extra-regional material. *Sed*aDNA is sufficiently preserved under cold conditions (Willerslev et al., 2014; Parducci et al., 2017), and DNA leaching is not reported from lake sediments (Sjögren et al., 2017). *Sed*aDNA allows for the identification of a higher number of plants per sample than other palaeoecological methods, and it generally reflects the catchment plant diversity rather than regional diversity (Sjögren et al., 2017; Parducci et al., 2019; Liu et al., 2020). However, *sed*aDNA analyses often give results as a mixture of plant types, as relative plants commonly share parts of their genome.

The palaeobotanical studies of *sed*aDNA are mostly based on the enrichment of a plant-specific, short barcode marker (P6 loop of the trnL (UAA) intron) located on the chloroplast genome (Taberlet et al., 2007; Capo et al., 2021; Revéret et al., 2023). An increasing number of *sed*aDNA studies are available from high-latitude regions, both from lake cores and permafrost samples (Revéret et al., 2023; Williams et al., 2023). *Sed*aDNA studies revealed temporal changes in plant diversity in the Russian polar territories: for example, in Buor Khaya Peninsula, the East Siberia (Zimmermann et al., 2017a), in Yakutia (Liu et al., 2020), in the Taymyr Peninsula (Jørgensen et al., 2012; Niemeyer et al., 2017), in the Anadyr Mountains (Huang et al., 2021), on the Bol'shoy Lyakhovsky Island (New Siberian Archipelago: Zimmermann et al., 2017b), and in the Polar Ural Mountains (e.g., Clarke et al., 2019, 2020; Bjune et al., 2021). The papers provide evidence of long-term persistence of arctic–alpine and boreal species through the climate changes, although they also document a decline in plant diversity during the past expansion of woody vegetation.

Willerslev et al. (2014) performed ancient DNA-based circumpolar research, providing 50 000 years of the Arctic vegetation history. On the global scale, they described the vegetation as consisting of dry steppe–tundra dominated by forbs for much of their investigated period, with a marked decline in diversity during the Last Glacial Maximum (25–15 kyr BP) and changes to moist tundra dominated by woody shrubs and graminoids after ca 10 000 a BP. Furthermore, lakes in Northern Fennoscandia have been studied (Parducci et al., 2015; Clarke et al., 2019; Alsos et al., 2020, 2022; Revéret et al., 2023; Rijal et al., 2021). These works demonstrate a clear increasing gradient from Northern Fennoscandia eastward to the unglaciated areas of Northern Russia and Siberia. The authors show continuous regional records and provide good taxonomical resolution, proving that, although *sed*aDNA cannot fully resolve all peculiarities of the taxonomic structure and temporal dynamics of the past plant communities, it can improve the documentation of plant persistence throughout time.

As for the Kola Peninsula, up to now, studies involving *sed*aDNA are limited to the only publication (Wang et al., 2021) mentioning a single site in the Northern coast, that is, the Cape Svyatoy Nos (68°01′58″ N, 39°52′25″ E, 290 km northeast of lake Imandra; referred to as the "Cape Svyatoi") in the original publication, where the authors studied the permafrost samples (Wang et al., 2021). Along with the palaeoclimate, animal and human distribution niche modelling, the paper discusses changes in vegetation and climate at the pan-Arctic scale and is based on the 535 samples, including, together with Cape Svyatoy Nos, other 73 sites, the North Atlantic, North America, and Siberian coasts. The study does not give environment changes or vegetation history specifically for the Kola Peninsula at any resolution, using the sediments from the regional site only in the context of the whole transect.

Another attempt to study *sed*aDNA from peat samples of the Seida site, located in a discontinuous permafrost region in Northeastern European Russia, was described by Parducci et al. (2015). The Seida site is situated some 2000 km east of the study site. Virtually, we have not had any DNA-based palaeoecological research for the Kola Peninsula up to now. So far, there are no other studies from the whole of Northwestern Russia as well. In this paper, by performing *sed*aDNA analysis in the relatively well palynologically and palaeobotanically known region, we expect to provide higher floristic resolution in comparison to the previous records in the Kola Peninsula on the levels of regionally important plant

© 2025 The Authors *Journal of Quaternary Science* Published by John Wiley & Sons Ltd. 

species and genera, which are usually not or not often seen in the pollen records and to assess more details on the temporal dynamics of these taxa. We aim to (1) reveal the patterns of the regional flora during the last ca 13 300 a BP; (2) reconstruct vegetation and environment patterns in coherence with the regional climatic oscillations; and (3) track the main stages of the plant colonisation of the study area.

## Study area

### *General characteristics*

Lake Imandra (in Russian: озеро Имандра) is situated in the central part of the Kola Peninsula in Northwestern Russia (67°40′ N; 33°00′ E; Fig. 1(A)) within the Lake Grater (Bolshaya) Imandra depression, about 6 km from the nearest shore of the lake (Fig. 1(B)). It is the largest lake of the region in terms of both lake size (815 km$^2$ excluding the surface of isles) and catchment size (ca 12 300 km$^2$, see Fig. 2 in Lenz et al., 2020; the Russian State Water Register (2009; http://textual.ru/gvr/index.php?card=155366). The maximal and mean depths are about 67 m and 14.513–16 m, respectively. Its length is 109 km and its width varies from 9 to 20 km. The lake has a blade-shaped form, a complex shoreline and about 140 isles of different size as well as about 60 bays incised deep into the land (Fig. 1). The lake consists of three semi-isolated parts, namely (1) Bolshaya, or Khibinskaya Imandra in the North (area 328 km$^2$, length about 55 km, width 3–5 km); (2) Ekostrovskaya Imandra in the central part (area 351 km$^2$); and (3) Babinskaya Imandra in the west (area 133 km$^2$), which are connected by narrow straits and passages (e.g., Nikolaeva et al., 2017a, 2018). A number of rivers and streams outflow from Imandra and drain into the Kandalaksha Gulf of the White Sea, with the Niva River being the greatest one (Elshin, 1969). The Imandra Lake system developed from a periglacial water reservoir that was formed during the Valdaian (Weichselian; ca 115 000–ca 11 700 a ago) glaciation (Nikolaeva et al., 2017b; Boyes et al., 2021, 2023).

The area is built up of crystalline rocks (gneisses, plagiogneisses, migmatites, gneiss-granites, and amphibolites), formed in the Early Proterozoic, those are part of the White Sea geological block (composite terrane) (Mitrofanov, 1995, 2001). The valleys and topographic lows are filled up by loose Quaternary tills, fluvioglacial, subordinate alluvial, lacustrine, colluvial, and biogenic sediments (Niemelä, 1993). The lake depression and the surrounding area are influenced by neotectonic motions (e.g., Armand and Samsonova, 1969; Nikolaeva, 2001; Shvarev, 2003; Zykov, 2001).

### *Climate*

The climate at Lake Imandra is characterised by a mean annual temperature of about 0.5°C, an annual precipitation of about 853 mm, and an air humidity as high as 80.5% (Moiseenko et al., 2009). The mean temperature of January varies from −13°C to −15°C, while that of July is between 13°C and 15°C. Snow cover lasts up to 250 days. The mean wind speed is 4 m/s; strong winds (>15 m/s) and temperatures below 0°C can occur at any time of the year.

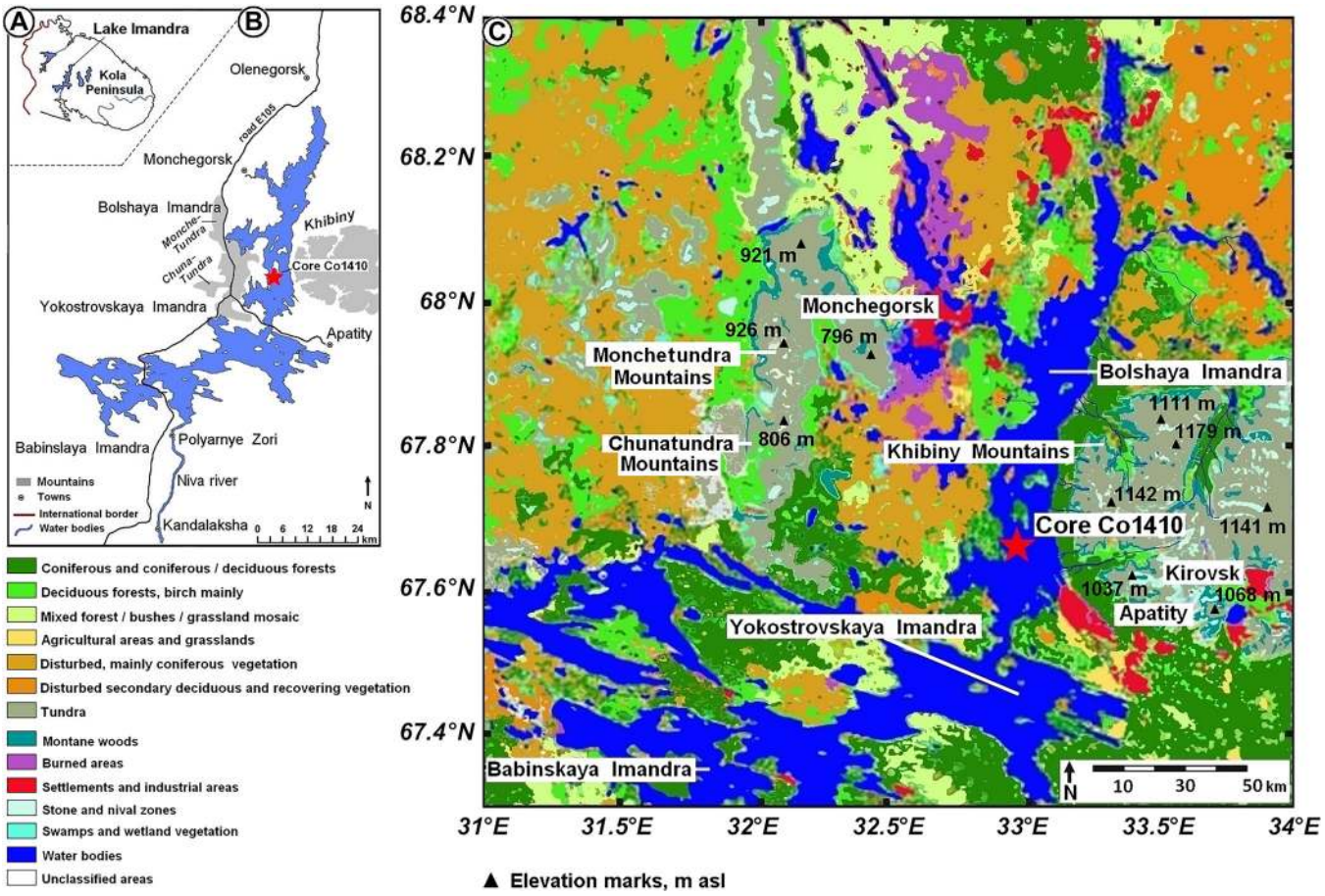



**Figure 1.** (A) Location of Lake Imandra on the Kola Peninsula. (B) Area of the Lake Imandra with settlements larger than 10 000 inhabitants, mountain regions (in grey), main rivers of the region, and the three sub-basins shown from the North to the South: Bolshaya or Greater Imandra, Yokostrovskaya Imandra, and Babinskaya Imandra. (C) Main vegetation and landscape types of the study area. Coring location is indicated with the red star. [Color figure can be viewed at wileyonlinelibrary.com]

© 2025 The Authors *Journal of Quaternary Science* Published by John Wiley & Sons Ltd.

### *Hydrographical conditions, water trophic state, and human impact*

Prior to the 1930s, Lake Imandra was described as a typical oligothrophic lake with low concentrations of suspended material (0.7–1.0 mg/L) and microelements (<1 μg/L, Moiseenko et al., 2009). Total phosphorus was less than 2 μg/L, and phosphates produced in the period of vegetation growth were completely utilised in production processes. Water transparency was about 7–8 m. The lake water was characterised by high oxygen saturation (to the bottom) due to high water inflow from mountain rivers. There was no stratification owing to wind turbulence during the ice-free period (e.g., Elshin, 1969; Moiseenko et al., 2009).

Lately, during the period from the 30 s to 90 s of the XX century, it has become a subject of greater levels of pollution. Industrial mining of copper- and nickel-rich apatite–nephelinite and iron deposits in the catchment area of Lake Imandra began in the 1930s. Considerable industrial expansion in the early 1900s resulted in the building of industrial enterprises in the lake catchment. As a consequence, large amounts of pollutants entered the lake between 1940 and 1990. The main pollution agents were heavy metals (predominantly nickel and copper), sulphates, chlorides, and nutrients, with the main pollution rates affecting the Northern part of the lake, namely the Great Imandra (Moiseenko et al., 2009). The transformation of economic conditions at the beginning of the 1990s caused a stop to many industrial activities in the Murmansk region, and, accordingly, slowed down lake pollution (e.g., Moiseenko and Yakovlev 1990; Moiseenko et al., 2009; Moiseenko et al., 2018). In the 2000s, environmental protection measures were taken; however, the lake still experienced high human impact, both industrial and recreational. By that, Lake Imandra represents a typical example of anthropogenic modification of an Arctic lake ecosystem and provides an opportunity to study its history and transformation.

### *Vegetation*

The study area lies within the northern boreal forest, and the main vegetation formations belong to the mixed coniferous pine and spruce forests (Fig. 1(C)). Norwegian spruce (*Picea abies* (L.) H. Karst./*Picea fennica* (Regel) Kom.) is a late-successional species in the Kola Peninsula, and it tends to form a treeline in the mountains (e.g., Orlova et al., 2013). Spruce forests with ericoid dwarf shrubs (e.g., *Ledum palustris* L., *Vaccinium myrtillus* L., *Vaccinium vitis-idea* L., *Vaccinium uliginosum* L., *Empetrum hermaphroditum* Hagerup), and mosses, mainly with *Pleurosium schreberi* (Brid.) Mitt.), dominate within the area. Mixed spruce and pine (*Pinus sylvestris* L./*P. fresiana* Wich) forests with the same species of dwarf shrubs and with *Chamaepericlimenum suecicum* (L.) Graebn. are less often observed. Pine forests and pine stands with lichens (*Cladonia mitis* Sandst., *Cladonia rangiferina* (L.) Weber ex F.H.Wigg., *Cladonia amaurocraea* (Flörke) Schaerer. and *Cetraria islandica* (L.) Ach.) are found in the drier areas. Birch (*Betula pubescens* Ehrh.) is a common component of forests. It tends to occur together with *Salix* spp. at disturbed areas as a secondary growth, along the water streams, and the nearby small lakes in the Imandra basin. It is found in the swamps and mires together with single trees of pine, *Betula nana* L., *Empetrum, Calluna vulgaris* (L.) Hull, *Vaccinium uliginosum* L., *Rubus chamaemorus* L., *Carex* spp. and *Sphagnum* spp. Besides, *Betula pubescens* Ehrh. and *Juniperus communis* L. can be components of the coniferous forests and make crooked stands at elevations higher than 400 m. According to Petrova and Razumovskaya (2017), the flora of aquatic plants includes 59 species of higher plants from 21 families. The main types of vegetation are depicted in the map (Fig. 1(C)). Data on vegetation are derived from the Landsat satellite images (1999–2017) and the own field data of A. Poliakova collected in 1999–2017.

## Materials and methods

### *Sediment coring and subsampling*

The study area is located in the southern part of the western flank of Lake Great (Bolshaya) Imandra (Fig. 1(B)). Sediment coring was carried out in summer 2017 at site Co1410 in the central part of the northern basin of Lake Imandra (67°42′57″ N, 33°05′06″ E; Fig. 1(C)) at ca 23 m water depth (maximal depth of the lake is 67 m with mean depth being ca 13 m; Moiseenko et al., 2009). The coring site was selected based on the local bottom orography and hydrological conditions as well as on the hydro-acoustic survey (for details see Lenz et al., 2020). At site Co1410, two parallel sediment cores, 7.98 and 8.65 m in length, respectively, were retrieved only a few metres apart. Coring was performed from an anchored platform using a gravity-corer in order to retrieve undisturbed near-surface sediments and a percussion piston-corer with a 2-m-long core barrel for deeper sediments (all UWITEC, Austria). After recovery, the cores were split into up to 1-m-long sections, packed, sealed, and kept at low temperatures (about 4°C) in the dark conditions during transport and storage. In the laboratory, the core was cut lengthwise and described for sedimentary structures, colour (Munsell Soil Colour Chart), and sediment composition (smear-slide microscopy). One core half was sampled at a resolution of 0.02 m following the clean sampling procedures described by Pedersen et al. (2016) and keeping the same intervals along the entire core; aliquots of larger samples were transported to the Tromsø University Museum, at UiT—The Arctic University of Norway, where they were stored frozen (−18°C) until further processing in 2019–2021.

### *DNA extraction, PCR amplifications, and sequencing*

DNA analyses were performed in the dedicated ancient DNA laboratory at the Arctic University Museum, Tromsø, Norway. DNA was extracted using DNeasy PowerLyzer PowerSoil Kit (Qiagen) and incorporating a bead beating step as described in Alsos et al. (2020) and Poliakova et al. (in preparation). Negative controls were included during sampling from the core (separate control for each batch of 10 samples), extraction, and PCR setup, as well as positive controls during PCR. In total, 81 samples, six extraction controls, nine PCR negative controls, and three PCR positive controls were analysed. Bench control (extra-clean Millipore water, molecular biology standard) was used when performing DNA extraction, and hood control was applied when preparing PCR plates for each batch of sediment samples. In addition, a negative post-PCR laboratory control was used to control the reagent and in-laboratory contamination. Post-PCR lab PCR positive control (synthetic standard) was applied at the step of DNA amplification to control the overall quality of the reaction (for details see Supporting material: Table S1, datasheet: Negative_&_Positive_Control).

We amplified the short and variable P6 loop region of the chloroplast *trn*L (UAA) intron (Taberlet et al., 2007), following the same analysis protocol (Alsos et al., 2020, 2016; Sjögren et al., 2017), and running eight PCR replicates on each DNA

© 2025 The Authors *Journal of Quaternary Science* Published by John Wiley & Sons Ltd. 

extract using unique 8 or 9 bp long tags added to the 5′ end of each primer. We pooled the PCR replicates and thereafter cleaned and quantified them using Qubit (Invitrogen™ Quant-iT™ and Qubit™ dsDNA HS Assay Kit, Thermofisher). Then we converted the pools into DNA libraries using a Truseq DNA PCR-free low-throughout library prep kit (Illumina). The library was quantified by qPCR using the KAPA Library Quantification Kit for Illumina sequencing platforms (Roche) and a Prism 7500 Real Time PCR System (Life Technologies, Fisheries faculty, UiT). The library was normalised to a working concentration of 10 nM using the molarity calculated from qPCR adjusted for fragment size. Sequencing was conducted on an Illumina NextSeq. 500 platform (2 × 150 bp, mid-output mode, dual indexing) at the Genomics Support Centre Tromsø (UiT).

## DNA sequencing analyses and filtering

The next-generation sequencing data were aligned, filtered, and trimmed using the OBITools software package (Boyer et al., 2016) and a custom R script (available at https://github.com/Y-Lammers/MergeAndFilter). We used the local circumarctic/circumboreal ArcBorBryo library containing 2445 sequences of 815 arctic and 835 boreal vascular plants as well as 455 bryophytes (Soininen et al., 2015; Sønstebø et al., 2010; Willerslev et al., 2014). In addition, a global reference library was obtained by running the *ecotag* programme on the EMBL (rl143) nucleotide reference database. We only retained sequences that 100% matched one of the reference libraries and had a minimum of three replicates across the dataset.

We manually cross-checked those identifications to ensure they were consistent between the regional and global reference libraries. In addition, NCBI BLAST was used to cross-check the identification of sequences with inconsistent taxonomic assignments. For sequences assigned to several taxa, the most likely taxa with 100% match were listed based on known presence in the native flora (Gorodkov, 1953; Mishkin, 1953; Kuzeneva, 1963; Poyarkova, 1954, 1956, 1959, 1966; Gribova et al., 1980; Kozhin et al., 2020). In cases where several sequences were assigned to the same taxon, we merged them only if they mainly occurred in the same samples. Details on the taxa identified in metabarcoding of *sed*aDNA from Lake Imandra (Kola Peninsula, Northwest Russia) can be found in the Supporting material (Table S1, datasheet: List of taxa with assignments and Table S1, datasheet: Sequences with comments).

## Stratigraphic diagrams and zonation

Stratigraphic diagrams were prepared using the TILIA/TILIA.GRAPH software (Grimm, 1990, 1992, 2004). The diagrams were subdivided into local zones, which were established based on comparing principal taxa and group dynamics, supported by the results of the depth-constrained cluster analysis by sum-of-squares implemented with CONISS for TILIA (Grimm, 1987). In addition, OPTIMAL DIVISION (Gordon and Birks, 1972) was used. Zones on the diagrams were only accepted if there was a consensus between zonation methods. The stability of the classification and the sharpness (probability, $p$; $1 \leq p > 0$) of the clusters were tested using the bootstrap resampling performed in MULTIV (Pillar and Orlóci, 1996; Pillar, 1999).

Eight ecological groups of identified plants were established:

1. Trees and shrubs include woody plants of both coniferous and deciduous types, that is, *Picea obovata, Pinus sylvestris, Juniperus communis, Betula pubescens/B. nana* type, *Alnus incana/A. kolaensis* type, *Frangula alnus, Lonicera caerulea/L. subarctica* type, *Populus tremula, Prunus padus, Ribes* sp., *Salix* sp./*Populus* sp. type, and *Sorbus* sp./*Cotoniaster* sp. type.
2. Dwarf shrubs include woody plants with perennating buds borne close to the ground, that is, *Andromeda polifolia, Arctostaphylos uva-ursi, Arctous alpine, Calluna vulgaris, Chamaedaphne calyculata, Dryas octopetala/D. punktata* type, *Empetrum hermaphroditum, Kalmia procumbens, Oxycoccus microcarpus, Phyllodoce caerulea, Rhododendron tomentosum, Rubus* sp./*Fragaria* sp. type, *Vaccinium uliginosum*, and *V. vitis-idaea*.
3. Forbs include all flowering taxa of herbaceous plants known from regional flora from the families of, for example, Apiaceae, Asteraceae, Boraginaceae, Brassicaceae, Caprifoliaceae, Fabaceae, Geraniaceae, Lamiaceae, Onagraceae, Orobanchaceae, Polygonaceae, Ranunculaceae, Primulaceae, Saxifragaceae, Urticaceae, and Violaceae.
4. Graminoids included genera and, when applicable, species from the families of Cyperaceae, Juncaceae, and Poaceae.
5. The group of higher spore plants, that is, pteridophytes (HSP) is composed of ferns, *Lycopodium/Diphasiastrum* type, and *Equisetum*.
6. Bryophytes include a variety of mosses.
7. Aquatic plants include all taxa growing in the lake water body as well as on the wet coasts. This group includes both high aquatic plants (HAP), for example, *Callitriche, Caltha, Hippuris, Myriophyllum, Nuphar* sp./*Nymphaea* sp., *Potamogeton* species and *Stuckenia*, as well as algae, that is, *Closterium baillyanum*, *Comarum palustre*, and *Nannochloropsis*.
8. Exotic and excluded types include plants that are not known from local and/or regional natural flora, for example, *Tilia* sp., *Quercus* sp., *Theobroma cacao,* and *Ocimum basilicum,* which are known as common contaminants of the reagent and laboratory. These plants were included in the calculations of the identified number of taxa but were excluded from any further analysis, as these plants are irrelevant to the modern and/or any of the past floras.

To study geographical patterns of the palaeofloras, all taxa were assigned to the groups according to their presence and frequency in the biogeographic regions and bioclimatic zones (according to their assignment by Elven et al., 2011 and PAF, 2011; http://panarcticflora.org/). Each plant identified in the *sed*aDNA record was assigned to a certain group according to the authors of primary sources, namely circumpolar–alpine, circumboreal, circumboreal–polar, boreal–nemoral and multizonal taxa. "Circumboreal taxa" occur more or less continuously throughout the boreal and often in the temperate parts of Eurasia and North America (sometimes including southern Greenland). "Circumboreal–polar" combines circumboreal and circumpolar patterns; they are distributed from boreal/temperate to arctic "circumpolar–alpine" zones and have circumpolar distribution with occurrences in one or more temperate mountain ranges south of the boreal zone. "Boreal–nemoral" plants refer to taxa characteristic of both boreal and broad-leaved temperate deciduous forest (i.e., nemoral) forest. We also introduced the category "multizonal" for plants that are widespread and present in more than two of the abovementioned zones. Treating these plants separately provides a clearer picture of the local flora and vegetation development in terms of their response to the changing temperature and the overall climate dynamics.

## Detrended correspondence analysis

To study taxonomic composition of the floristic spectra revealed by *sed*aDNA analysis of the core Co1410 from Imandra lake throughout the time, detrended correspondence analysis (DCA, Hill and Gauch, 1980) was carried out using

© 2025 The Authors *Journal of Quaternary Science* Published by John Wiley & Sons Ltd. 

the programmes Canoco for Windows 4.5 and CanoDraw for Windows 4.13 (ter Braak and Šmilauer, 2002). All taxa with 100% match to the reference libraries were included in the analysis with exception of exotic plants. All taxonomic data were standardised by the logarithmic transformation, which removes the bias from highly dominant taxa and improves the fit of the count data. Evaluation of the significance of the DCA axes was performed by the null hypothesis testing using the nonparametric Monte Carlo permutation test (Manly, 1992). Under the null hypothesis, we expected that no relations exist between the variation in taxonomical composition and the sediment depth. After the tests rejected the null hypothesis, calculation of the length of the environmental gradient was performed in order to decide on the appropriate statistical method for further analysis (as recommended by Hill and Gauch (1980) and ter Braak and Šmilauer (2002).

### *Core imaging and age-depth model*

Based on line-scan images, core description, and selected XRF data, the core segments were merged using the Corelyzer 2.0.4 software (National Lacustrine Core Facility, LacCore, and Continental Scientific Drilling Coordination Office, CSDCO), resulting in a spliced 8.46-m-long master record Co1410 (Lenz et al., 2020). The chronology of the core Co1410 from Lake Imandra is based on six radiocarbon (14 C) samples of organic macroremains (for details see Lenz et al., 2020). Samples were prepared as described in Rethemeyer et al. (2013) and Lenz et al. (2020) and measured by accelerator mass spectrometry (AMS) using the CologneAMS facility (Dewald et al., 2013). The 14 C ages were converted to calibrated years before AD 1950 (cal a BP) using the software OxCal v4.4 (Bronk Ramsey, 1994, 1995; Heaton et al., 2020; Reimer et al., 2020) based on the IntCal13 atmospheric calibration curve for the Northern hemisphere (Reimer et al., 2013). The age-depth model was simulated using the "rBacon" library (Blaauw and Christen 2011; Blaauw et al., 2020) for R (R Development Core Team, 2017). The detailed process of establishing the chronology is described in Lenz et al., 2020. Working on the same sediment cores, we adopted their age-depth for the present studies: the age-depth model, reproduced with small additions, is given in the Supporting materials S2: Age-depth model of the sediment profile Co1410, based on six $^{14}$C ages derived from organic macroremains and additional tie points from $^{137}$Cs and Hg measurements as well as pollen stratigraphy with the upper and lower boundary of the Younger Dryas according to Lohne et al. (2013) for Northern Europe (i.e., 12 710 ± 52 cal a BP and 11 546 ± 59 cal a BP, respectively). The Younger Dryas and Holocene boundary, in addition, is supported by the previous studies performed by Brauer et al. (1999), that is, 11 590 ± 40 a BP.

The ages of the record are discussed in this work as time windows in order to minimise the error due to the uncertainty of the age-depth model. In the upper part, two tie points from the sediment–water interface, $^{137}$Cs and Hg measurements, and radiocarbon dating were included in the age-depth model. In the lower part, two tie points were derived for Allerød/Younger Dryas (12 710 ± 52 cal a BP; Lohne et al., 2013; Lenz et al., 2020) and for the Younger Dryas/Holocene boundaries (11 546 ± 59 cal a BP; Brauer et al., 1999; Lohne et al., 2013; Lenz et al., 2020). Tie points and radiocarbon data obtained from Co1410 are given in Table 1 in Lenz et al. (2020).

## Results

In total, 11 178 580 reads of 311 sequences match 100% to the reference libraries, that is, ArcBorBryo (Sønstebø et al., 2010; Willerslev et al., 2014; Soininen et al., 2015) and the reference library of the National Centre for Biotechnology Information (NCBI). We estimated 227 matches to ArcBorBryo, 302 to NCBI, and 218 to both libraries. Among reads with a total of <10 repeats and <1000 reads, there were 5912 reads of 44 sequences with 100% match only to NCBI. The majority of them were only identified to the above species level, and all except nine had a homopolymer region. As they represent less than 0.05% of the identified sequences and the majority likely reflect natural sequence variation or PCR/sequencing error, these sequences were discarded. The remaining dataset consisted of 11 172 668 reads of 267 sequences. After discarding 19 sequences that were suspected false positives, and merging sequences assigned to the same taxon, our final dataset consists of 10 975 217 reads of 223 taxa (see Supporting material S1, datasheet: Total reeds).

Most *sed*aDNA samples from core Co1410 allowed to identify 53.8 ± 28.4 plant taxa on average. The maximal taxa (110 101 reads and 100 taxa) were registered from the samples of 0.28 m (−2 cal a BP or ca 1948 CE), 0.96 m (1090 cal a BP), and 3.20 m (5870 cal a BP), respectively. Two samples (from the core depth of 0.56 m, that is, ca 380 cal a BP and from the depth of 5.74 m, i.e., 11 900 cal a BP) yielded the least amount of DNA (68 346 and 64 265 sums of total reads respectively) and were omitted from the further taxonomical and phytogeographical analysis. Complete list of identified plants is available in the Supporting material S1, datasheet: List of taxa with assignments and diagram from S4: Phylogenetic relationship of identified taxa.

### *sedaDNA stratification, local palaeo-zones, and dynamics of taxonomic diversity*

Five local palaeoecological zones (Co-1 to Co-5, Figs. 2 and 3) meeting statistical criteria $p \geq 0.6$ (probability; $1 \leq p > 0$) are described based on the constrained hierarchical cluster analysis of Bray–Curtis community distance on PCR replicates per sample and the comparison with the analysis based on Euclidian distance and a broken stick model distribution. Besides, two subzones are established in the first and the last palaeo-zones, Co-1a ($p = 0.72$) and Co-1b ($p = 0.68$); Co-5a and Co-5b, respectively ($p = 0.65$ for both). Cluster analysis (Figs. 2 and 3) as well as PCA ordination also suggests

**Table 1.** Local *sed*aDNA zones in the sediment sequence Co-1410 with age frames, total number of identified taxa, and the dominating type of palaeo-vegetation.

| Zone (subzone) | Depths, m | Ages ± error, cal a BP | Number of taxa | Dominating type in palaeo-vegetation |
|---|---|---|---|---|
| Co-5 | 0.04–0.56 | −70 ± 1–520 ± 30 | 162 | Coniferous forest with dwarf shrubs |
| Co-4 | 0.64–2.94 | 520 ± 30–5490 ± 120 | 177 | Mixed coniferous/deciduous forest |
| Co-3 | 3.04–4.02 | 5490 ± 120–8530 ± 160 | 141 | Deciduous (birch) forest with forbs |
| Co-2 | 4.34–5.26 | 8530 ± 160–11 820 ± 200 | 109 | Open grasslands |
| Co-1b | 5.46–7.70 | 11 820 ± 200–13 040 ± 830 | 82 | Open grasslands with forbs |
| Co-1a | 7.76–8.36 | 13 040 ± 830–13 300 ± 850 | 50 | Tundra with dwarf shrubs |

© 2025 The Authors *Journal of Quaternary Science* Published by John Wiley & Sons Ltd.

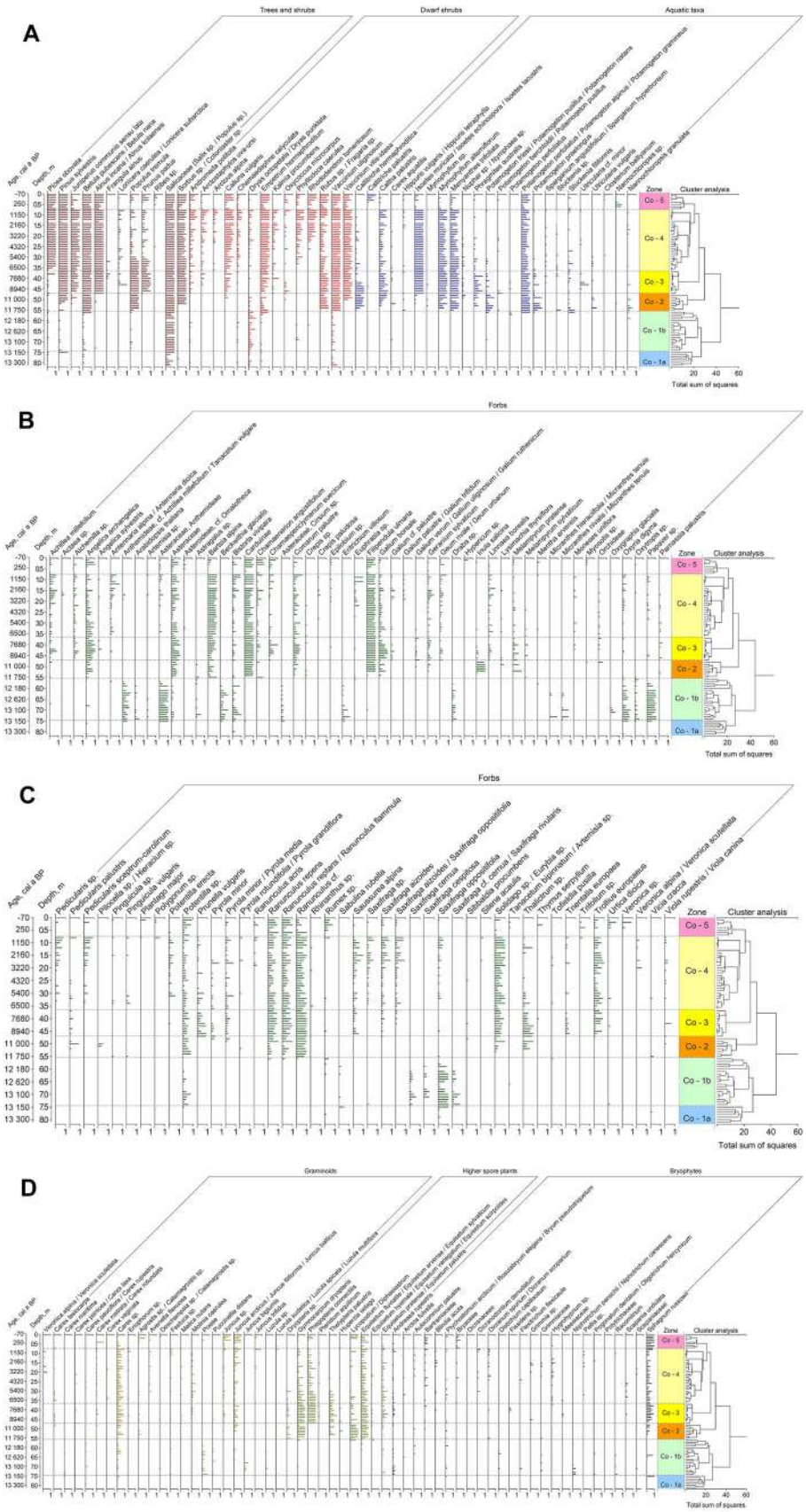



**Figure 2.** Stratigraphic diagram of (A) trees and shrubs (dark red), dwarf shrubs (red bars) and aquatic taxa: HAP (dark blue) and algae (light blue); (B and C) selected forbs (dark green bars) with the greatest abundances; (D) selected graminoids (dark ochre bars), HSP (yellowish-green bars), and bryophytes (dark grey bars) identified from *sed*aDNA in the core Co-1410, Imandra lake, central part of Kola Peninsula. The diagram shows the number of PCR replicates of identified taxa (bars; X-axis) corresponding to sample depth (m, 1st Y-axis) and age (cal a BP; 2nd Y-axis). The hatched lines mark five local *sed*aDNA zones (Co-1 to C-5) with two subzones in the first zone (Co-1a to Co-1b). Full list of taxa is available in the Supporting material S1. (A: Trees, shrubs, dwarfs, aquatic plants). (B: Forbs_beginning). (C: Forbs_end). (D: Graminoids and bryophytes). [Color figure can be viewed at wileyonlinelibrary.com]

subzones for Co-3 and Co-4 local palaeo-zones; however, their acceptance is statistically disapproved ($p < 50$ for both). The greatest assembly distance among samples was between those from depths 8.36 m and 5.46 m (13 300 and 11 800 cal a BP, respectively), making the oldest zone the most distinct. The identified *sed*aDNA zones are clearly reflected by the taxa and vegetation groups dynamic in the *sed*aDNA data (Figs. 2 and 3; Table 1).

The smallest taxa diversity is described for the oldest zone Co-1: Subzone Co-1a (50 identified taxa) is characterised by

© 2025 The Authors *Journal of Quaternary Science* Published by John Wiley & Sons Ltd.

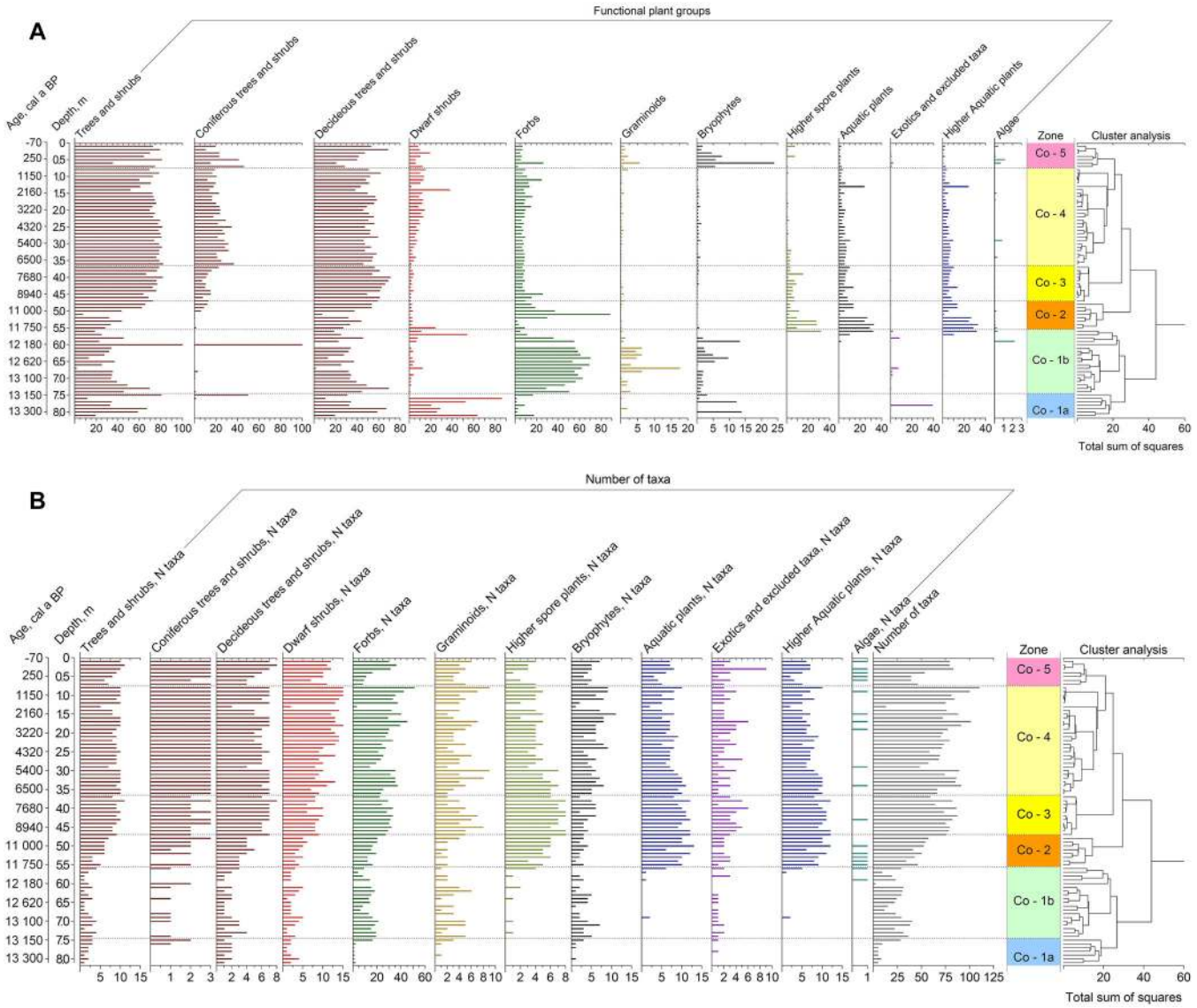



**Figure 3.** Stratigraphic diagram showing (A) proportions of the main vegetation functional groups: trees and shrubs (dark red bars); dwarf shrubs (red bars); forbs (dark green bars); graminoids (dark ochre bars); bryophytes (dark grey bars); HSP (yellowish-green bars); aquatic plants in total; HAP (dark blue bars) and algae (light blue bars) as well as the proportions of exotic and excluded plants (purple) identified from *sed*aDNA in core Co1410. (B) Numbers of taxa identified within the main vegetation functional groups: trees and shrubs (dark red bars); dwarf shrubs (red bars); forbs (dark green bars); graminoids (dark ochre bars); bryophytes (dark grey bars); HSP (yellowish-green bars); aquatic plants in total; HAP (dark blue bars) and algae (light blue bars) as well as the proportions of exotic and excluded plants (purple) registered from *sed*aDNA in core Co1410. The diagram shows the percentages of the sum of the total reeds of identified taxa (bars; X-axis) corresponding to sample depth (m, 1st Y-axis) and age (cal a BP; 2nd Y-axis). The hatched lines mark five local *sed*aDNA zones (Co-1 to C-5) with two subzones in the first zone (Co-1a to Co-1b). (A: groups of identified plants). (B: number of identified plants). [Color figure can be viewed at wileyonlinelibrary.com]

the lowest numbers of recognised forbs (24), graminoids (7), bryophytes (6) and dwarf shrubs (5) as well as the absence of identified high spore and aquatic plants. Subzone Co-1b is characterised by some increased number of taxa within all functional groups (82 taxa are identified in total, Figs. 2 and 3(B)). With 30 forbs, 12 bryophytes (twice as many as in the previous subzone), 10 graminoids, and the occurrence of three aquatic plants: two HAP (*Carex aquatilis* and *Potamogeton friesii/Potamogeton pusillus/Potamogeton natans* type and *Nannochloropsis granulate*, the algae. HSPs are represented by *Gymnocarpium dryopteris*, *Equisetum fluviatile/Equisetum arvense/Equisetum sylvaticum* type, and *Equisetum pratense/Equisetum palustre*. Among dwarf shrubs, two species, *Phyllodoce caerulea and Rhododendron tomentosum,* occur in addition to previously present *Andromeda polifolia, Chamaedaphne calyculata, Dryas octopetala/Dryas punktata, Empetrum hermaphroditum*, and *Vaccinium uliginosum* (Fig. 3).

Floristic diversity in Co-2 further increases to 109 taxa with 43 forbs, reduced number of graminoids (6) and bryophytes (8), whereas the number of HAP increases strongly (up to 18 taxa). Number of dwarf shrubs is unchanged (7), but their spectrum is not the same: *Chamaedaphne calyculata, Phyllodoce caerulea,* and *Rhododendron tomentosum* are not encountered in this zone, whilst *Calluna vulgaris, Oxycoccus microcarpus, Rubus* sp./*Fragaria* sp. Type and *Vaccinium vitis-idaea* are identified for the first time in this core (Figs. 2 and 3(B)).

Further increase in diversity occurs in the Co-3 zone (141 taxa). The number of forbs is 53, HAP 20, and the number of graminoids and bryophytes is the same, 13. The number of dwarf shrubs is 11. *Andromeda polifolia* and *Chamaedaphne calyculata* recur after 4.02 m. *Arctostaphylos uva-ursi* and *Kalmia procumbens* are encountered for the first time.

In the zone Co-4, floristic diversity is the highest for the whole core (177 taxa). Forbs are represented by 73 taxa

© 2025 The Authors *Journal of Quaternary Science* Published by John Wiley & Sons Ltd. 

(20 more compared to zone Co-3, Figs. 2 and 3(B)), additionally, 21 bryophytes are encountered, 17 HAP, and 15 graminoids. All types of dwarf shrubs are found in this zone, including *Phyllodoce caerulea* re-occurring in this zone after 2.66 m and *Rhododendron tomentosum* re-occurring after 1.92 m. *Arctous alpine* appears for the first time at 2.94 m and is constantly present after 1.64 m. All 11 woody taxa constantly occur in this zone. After 2.56 m, *Frangula alnus* is not encountered.

The last stratigraphic zone, Co-5, shows a reduction of the floristic diversity (162 taxa). The number of forbs is about the same (70 taxa), the number of bryophytes is reduced to about one-fourth (15), and the number of graminoids and HAP is 14 for both. Woody taxa do not show any statistically significant change (Figs. 2, 3, and 4(B)).

## Taxonomic proportions of palaeofloras

In total, 223 taxa were identified. These taxa belong to 150 genera and 86 families (Fig. 4(A)). The resulting sequences were assigned to vascular plants (87%), algae (1%), and bryophytes (12%). About half (111 taxa, 49%) were identified to the level of species. Trees and woody shrubs account for 12 taxa (six of them are identified up to the level of species). Of the 15 dwarf shrubs identified, 12 are identified at a species level. Forbs (95 taxa identified, 50 species, 65 genera) showed the highest diversity.

From the graminoids, 22 taxa were identified in total, with 10 to the species level. HSP (five species out of 10 taxa) are represented by five ferns (*Dryopteris* sp., *Gymnocarpium dryopteris, Phegopteris connectilis, Pteridium aquilinum*, and *Thelypteris palustris*), three types of horsetails (*Equisetum fluviatile/Equisetum arvense/Equisetum sylvaticum, Equisetum hyemale/Equisetum variegatum/Equisetum scirpoides, and Equisetum pratense/Equisetum palustre*), as well as two homosporous clubmosses (*Huperzia selago* and *Lycopodium/Diphasiastrum*).

Among bryophytes, 27 taxa were registered (eight identified as species and 17 as genera). Aquatic plants (23 taxa in total, 13 species) predominate by HAP (20 taxa, 11 species), whereas the number of algae is three taxa only (*Closterium baillyanum, Nannochloropsis* sp., and *Nannochloropsis granulata*; Fig. 4(A)). In addition, a total of 19 exotic taxa were identified but not included into further analysis as these taxa are most likely false positives (e.g., contamination during the laboratory processing or as a part of reagents, or false match due to DNA reference library issues) and do not reflect local and/or regional flora.

Most of the taxa (143 of the total 223) were identified to the level of genera, with 66 forbs and 17 bryophytes among them. Among the 111 species detected, an additional 49 forbs and 13 aquatic plants were recognised. The remaining 84 taxa were identified not further than a family level, with 26 forbs and 17 bryophytes being the most abundant groups in each local palaeoecological zone (Fig. 4(A),(B)).

One taxon, Salicaceae (*Salix* sp./*Populus* sp. type), is present in almost all samples (80 out of 81). Further vascular plants abundant in the *sed*aDNA record are *Vaccinium uliginosum* (registered in 70 samples), *Betula* type (66), Asteraceae indet. (62), *Empetrum hermaphroditum* (60), *Potentilla* sp. (found in 60 samples). *Pinus sylvestris* was found in 59 samples. *Carex* sp. (58) is the most common graminoid. HSPs are most often represented by the *Equisetum fluviatile/Equisetum arvense/Equisetum sylvaticum* type (registered in 56 samples). As for HAP, *Potamogeton perfoliatus/Potamogeton alpinus/Potamogeton gramineus* was identified in 56 samples. Other taxa were registered in fewer than 55 samples. The most common moss is *Sphagnum russowii* (51). Algae were registered the least: among them, *Nannochloropsis granulata* was the most common, found in 12 samples. *Hypericum* sp. and indet taxa from Dicranaceae and Polytrichaceae families were registered in one sample only.

## Geographical proportions

Core Co1410 is dominated by taxa with multizonal distribution (131 types out of 204 identified taxa, or 64% of the total sum of PCR reads; Supporting material S1) with 61 of forbs, 24 bryophytes, 18 graminoids, 10 HAP, five HSP, and three algae (Fig. 4(C)). The group of circumboreal types (29 taxa or 14%) is built up mainly of forbs (10) with trees/tall shrubs (4), dwarf shrubs (4), and HSP (4) (Fig. 4(C)). Circumborea–polar taxa are built up with 21 taxa or 10%, to which HAP contribute seven types, forbs six, and dwarf shrubs four. Circumpolar–alpine (20 taxa or 10%) consists mainly of forbs (16) with dwarf shrubs and graminoids contributing two types each. Boreal–nemoral types comprise three taxa or 2% of the total sum of PCR reads: two forbs (*Chamaenerion angustifolium* and *Filipendula ulmaria*) and one tall shrub (*Frangula alnus*). This group is the least diverse and the least abundant one.

Multizonal taxa prevail in every stratigraphic *sed*aDNA palaeo-zone in core Co1410 (Fig. 4(D)). In **Co-1a**, their proportion is about 72%, followed by circumpolar–alpine (15%) and circumboreal–polar (11%) ones (Fig. 4(D)). In **Co-1b**, multizonal and circumboreal–polar taxa decrease to 61% and 4%, respectively, whereas the percentage of circumpolar–alpine taxa increases to 33%. In **Co-2**, multizonal taxa rise again to 70%, circumboreal–polar taxa come to the second position with 15%, and boreal–nemoral taxa add 9%, which is the highest rate in comparison to other zones and sub-zones (Fig. 4(D)). In zone **Co-3**, the percentage of multizonal taxa strongly decreases (to 49%), and a proportion of circumboreal–polar taxa increases up to 25%, with circumboreal taxa being about at the same rate (20%). Boreal–nemoral types add the next 3%. Zone **Co-4** is characterised by a higher abundance of multizonal taxa (53%) with equal contribution of circumboreal and circumboreal–polar taxa (both 22%). In the topmost **Co-5** zone, the proportion of multizonal taxa does not experience any strong change, about 57%, circumboreal–polar taxa add 23%, and some decreased proportion of circumboreal taxa gives an additional 18%. Contribution of both circumpolar–alpine and boreal–nemoral types is neglected (1% each, Fig. 4(D)).

## Results of DCA ordination

DCA ordination (Fig. 5) revealed an environmental gradient of 3.5 SD, suggesting a nonlinear distribution of data, with the first two dimensions of the DCA accounting for $\lambda1 = 56\%$ and $\lambda2 = 13\%$ of the total variance of *sed*aDNA data. The ratio $\lambda1 + \lambda2$/total variance, a measure of the goodness of fit equivalent to R2 (Jongman et al., 1987), is 0.86 (0.56 + 0.13/0.8). The relative distance between samples explains the differences in taxonomic composition revealed in the *sed*aDNA analysis. As shown in Figure 5(A), most of samples shown high correlation with the CONNISS clusters (Figs. 2 and 3), except the sample N60 (depth 58.8 m; reconstructed age of ca 12 000 a BP) as it was characterised by the lowest quality both in terms of DNA yield (proportion of PCR repeat is 0.125 that is one of eight repeats only) and the smallest taxonomic diversity (only two regionally known taxa, i.e., *Picea obovata* and *Pinus sylvestris*). This sample has, besides, 12 exotic taxa (plants not known regionally and irrelevant to the modern and/or any of the past floras, for example, *Theobroma cacao, Quercus* sp., *Ocimum*

© 2025 The Authors *Journal of Quaternary Science* Published by John Wiley & Sons Ltd. 

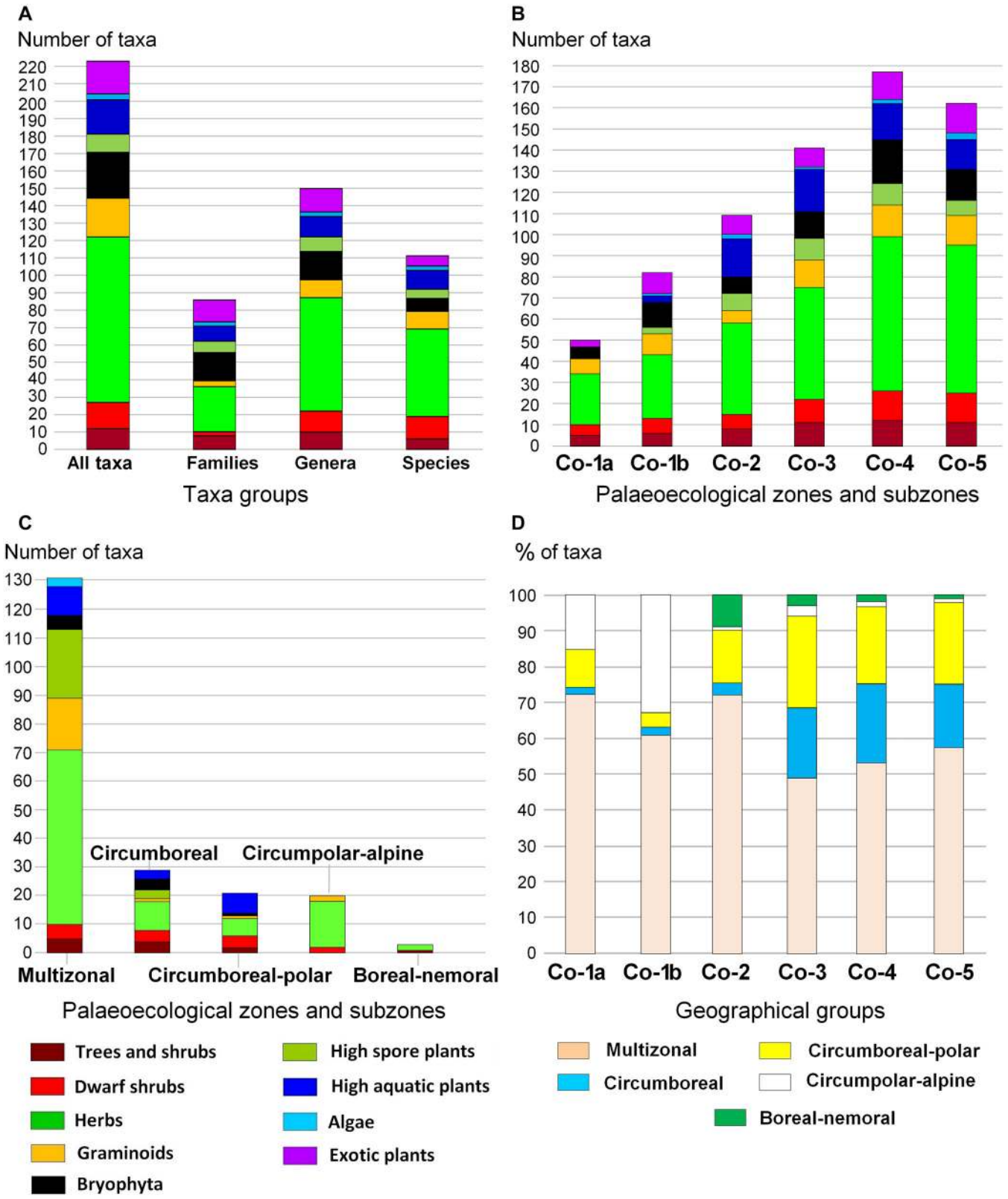



**Figure 4.** Number of taxa identified in the sediment core Co1410 in the *sed*aDMA analysis. (A) Diagram showing the number of all identified taxa, families, genera, and species. (B) Numbers of all identified taxa detected within the local palaeoecological zones and subzones. (C) Distribution of taxa belonging to different geographical groups (multizonal, circumboreal, circumboreal–polar, circumpolar–alpine and boreal–nemoral) in the local palaeoecological zones and subzones. (D) Distribution of functional vegetation groups among the geographical groups. Exotic plants were not included into analysis of geographical distribution (C–D). [Color figure can be viewed at wileyonlinelibrary.com]

*basilicum*). The same taxa were identified in comparable amounts in the negative control. These plants are most likely related to contamination; they are not seen in the samples from the depths above and below. Subzones Co-1a and Co-1b show the most distant position in comparison to other zones. Samples from the subzone Co-1b show no or very weak correlation with samples from zone Co-3 (mean $r^2 = 0.03$ to 0.12, $p < 0.001$), which suggests low ecological similarity.

Figure 5(B) shows a positive correlation between the samples NN 81-57 of Co-1 zone (7.76–5.46 m; ca 13 300–11 800 a BP) and mosses related to the Polytrichaceae family, as well as to

© 2025 The Authors *Journal of Quaternary Science* Published by John Wiley & Sons Ltd. 

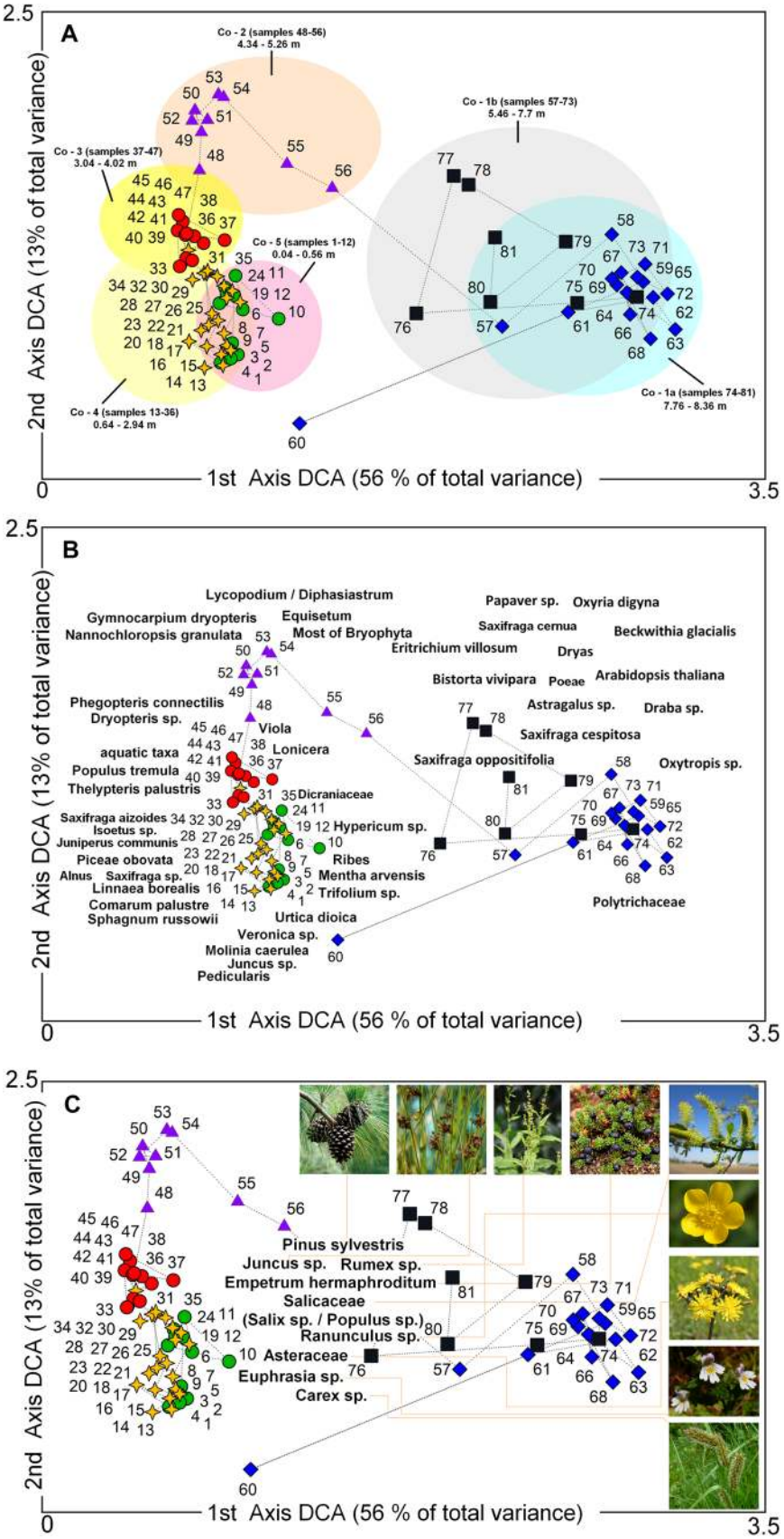



**Figure 5.** Results of detrended correspondence analysis (DCA) illustrating taxonomic composition of the floristic spectra revealed by *sed*aDNA analysis of core Co1410 from Imandra Lake. (A) Correlation of the sample depths and stratigraphic zones and subzones revealed by cluster analysis (Co-1a/b to Co-5). (B) Selected taxa show the most correlation to certain stratigraphic zones and subzones (Co-1a/b to Co-5). (C) Taxa showing no correlation to any of the stratigraphic zones and subzones (Co-1a/b to Co-5). Numbers 1–81 correspond to the sample numbers, core depths and sediment ages as following: NN 74–81 (7.76–8.36 m)—13 000–13 300 cal a BP; NN 57–73 (5.46–7.7 m)—11 800–13 000 cal a BP; NN 48–56 (4.34–5.26 m)—8500–11 800 cal a BP; NN 37–47 (3.04–4.02 m)—5500–8500 cal a BP; NN 13–36 (0.64–2.94 m)—520–5500 cal a BP; NN 1–12 (0.04–0.56 m)— −70–520 cal a BP. Plant taxa positions are in the middle of the related words. Scores for all taxa and samples are available in the Supporting material S4: Complete results of DCR analysis. [Color figure can be viewed at wileyonlinelibrary.com]

*Astragalus* sp., *Arabidopsis thaliana, Bartsia alpine, Beckwithia glacialis, Bistorta vivipara, Draba* sp., *Dryas,* and most of *Saxifraga* species, *Oxygraphis glacialis, Oxyria digyna,* and *Papaver* sp. *Eritrichium villosum* shows the highest correlation ($r^2 = 0.62$, $p < 0.001$) with the sample NN 68–73 (6.78–7.70 m; ca 12 400–13 000 a BP). Most of the bryophytes, all registered *Equisetum* taxa, *Lycopodium/Diphasiastrum, Gymnocarpium dryopteris,* are positively correlated with samples NN 56-48 from the zone Co-2 (4.34–5.26 m; ca 11 800–8500 a BP). Among aquatic taxa, *Menyanthes trifoliata, Potamogeton* sp., and algae *Nannochloropsis* sp. (including *Nannochloropsis granulata*) show distinct correlation to this zone, whereas almost all other aquatics show relation to the samples NN 47-37 from the next stratigraphic unit, Co-3 (3.04–4.02 m; ca 8500–5500 a BP).

© 2025 The Authors *Journal of Quaternary Science* Published by John Wiley & Sons Ltd.

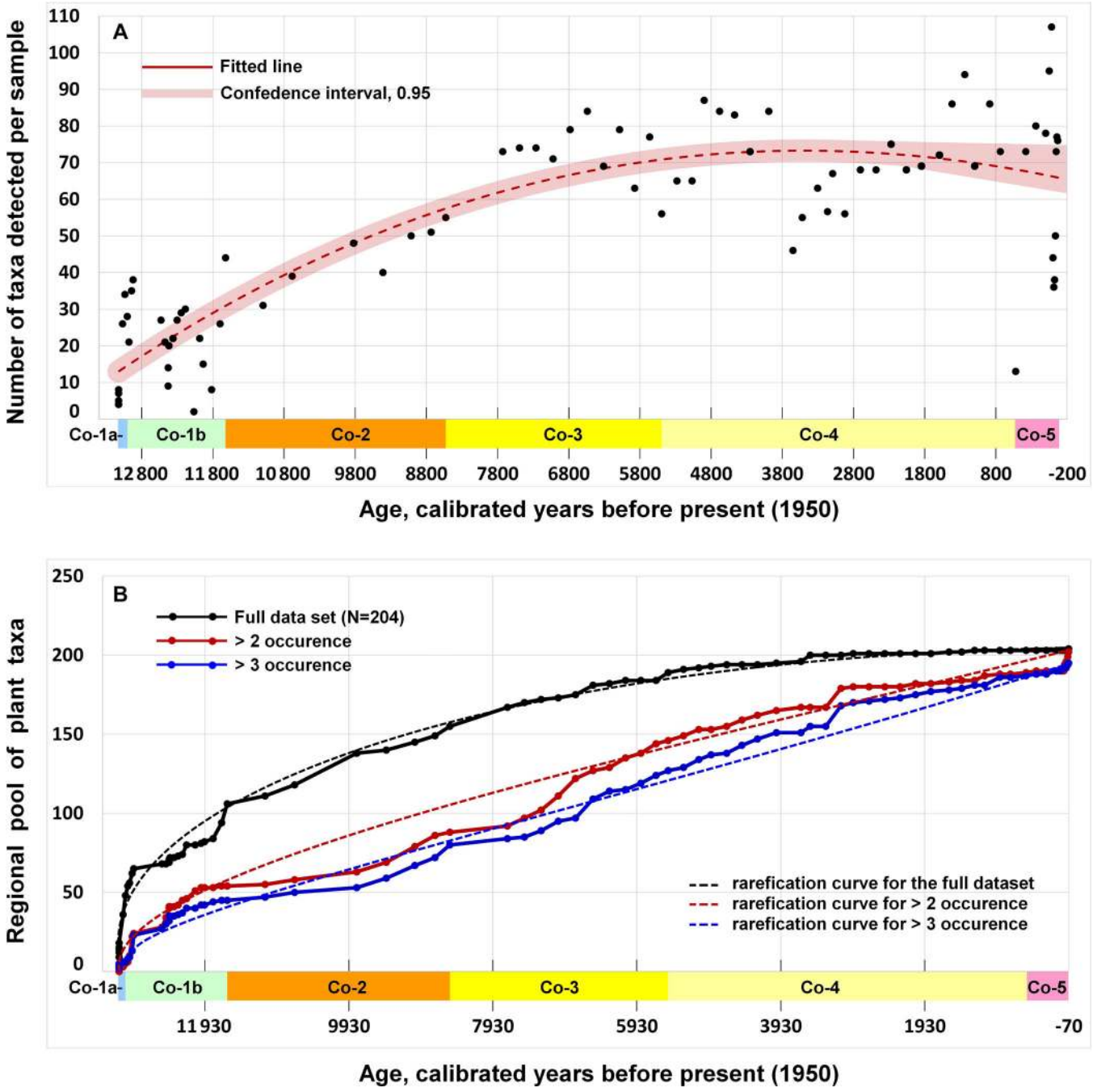



**Figure 6.** (A) Number of taxa detected per sample identified in the sediment core Co1410; (B) Regional pool of taxa accumulated during the last ca 13 300 a BP according to *sed*aDNA analysis. [Color figure can be viewed at wileyonlinelibrary.com]

Besides, most ferns, *Populus tremula, Frangula alnus, Filipendula ulmaria, Lonicera species,* and *Viola* sp. show a high positive correlation to this zone and are anticorrelated with the samples from zones Co-1 and Co-5. *Alnus species, Picea obovata*, and *Linnaea borealis* are correlated to samples NN 13-36 of palaeoecological zone Co-4 (0.64–2.94 m; 520–5500 a BP). *Sphagnum russowi, Hypericum* sp., *Mentha arvensis Pedicularis species, Ribes* sp., *Trifolium* sp., and *Urtica dioica* demonstrate strong (up to $r^2 = 0.9$, $p < 0.001$) correlation to the topmost samples, Co-5 (samples NN 1-12, ca 520 to −70 cal a BP).

In contrast, Astareceae, *Carex* sp., *Empetrum hermaphroditum, Euphrasia* sp., *Juncus* sp., *Pinus sylvestris, Ranunculus, Rumex* sp., Salicaceae (*Salix* sp./*Populus* sp.) do not show any statistically significant correlation to one or several stratigraphic zones or subzones (Fig. 5(C)). Those taxa are registered within all of the units with the exception of Co-1, where only DNA of Salicaceae is present consistently. For details on all taxa, consult Supporting material S4: Complete results of DCA.

## Discussion

### *Taxonomical sedaDNA spectra and comparison to current flora*

A high proportion (97%) of taxa identified in core Co1410 is also known from the present-day flora in the region. This suggests that by far most of the present-day flora in the catchment of Lake Imandra was already established during the phase of initial deglaciation, for example, sometime before 13 300 cal a BP. The reconstructed floras demonstrate a continuity in the taxonomic composition at least from the

© 2025 The Authors *Journal of Quaternary Science* Published by John Wiley & Sons Ltd.

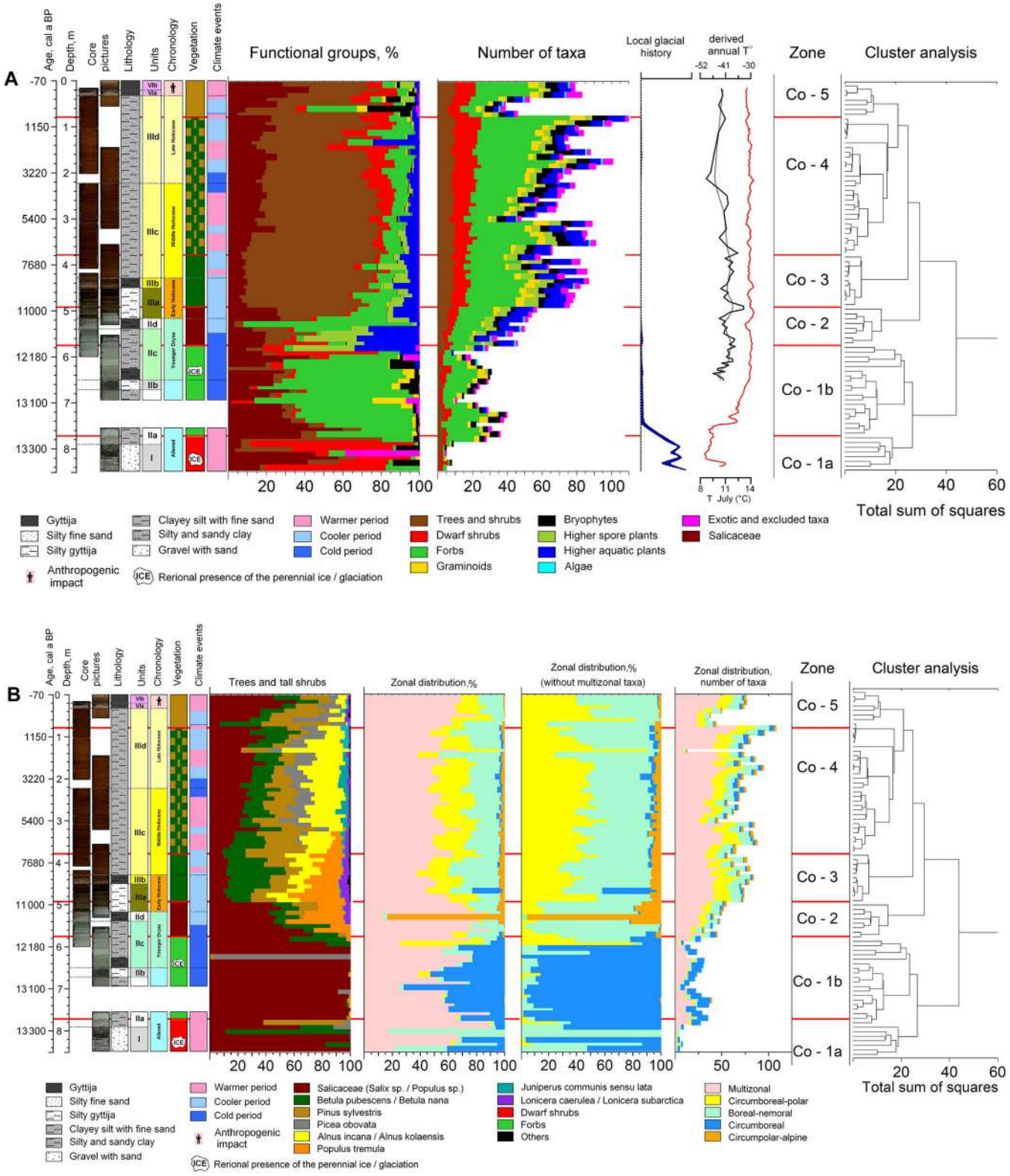



**Figure 7.** Line scan picture of the core Co1410, lithological and palaeoecological units, chronology, reconstructed type of the predominate vegetation, reconstructed climate events, 14 C dates, in comparison to (A) Changes in the dynamics of functional vegetation groups in total and related to terrestrial sum (aquatic and exotic taxa excluded), and dynamics of taxa number in comparison to the local glacial history and local reconstructed July temperature. Comparison to the local Scandinavian Ice Sheet (SIS) and mountain glacier histories reconstructed here (bluish shadings) as well as the local July temperature from Ilyashuk et al. (2013), the LOESS-smoothed record (span = 0.20, order = 1; grey line), and the d18O-derived annual temperature from the GISP2 ice core (Cuffey and Clow, 1997; Alley, 2000) using the calibration from Cuffey et al. (1995) (red line): data are adopted from Lenz et al., 2020. "ICE" stands for the presence of glaciers in the region. (B) Changes in the arboreal (trees and tall shrubs) vegetation in terms of dominating taxa and dynamics of the geographical types of plants (zonal distribution of taxa) in number of taxa and in percentage. Geographical types of plants are identified according Elven et al., 2011 and PAF, 2011; http://panarcticflora.org. (A) Dynamics of functional vegetation groups). (B) Dynamics of the geographical types of plants). [Color figure can be viewed at wileyonlinelibrary.com]

© 2025 The Authors *Journal of Quaternary Science* Published by John Wiley & Sons Ltd. 

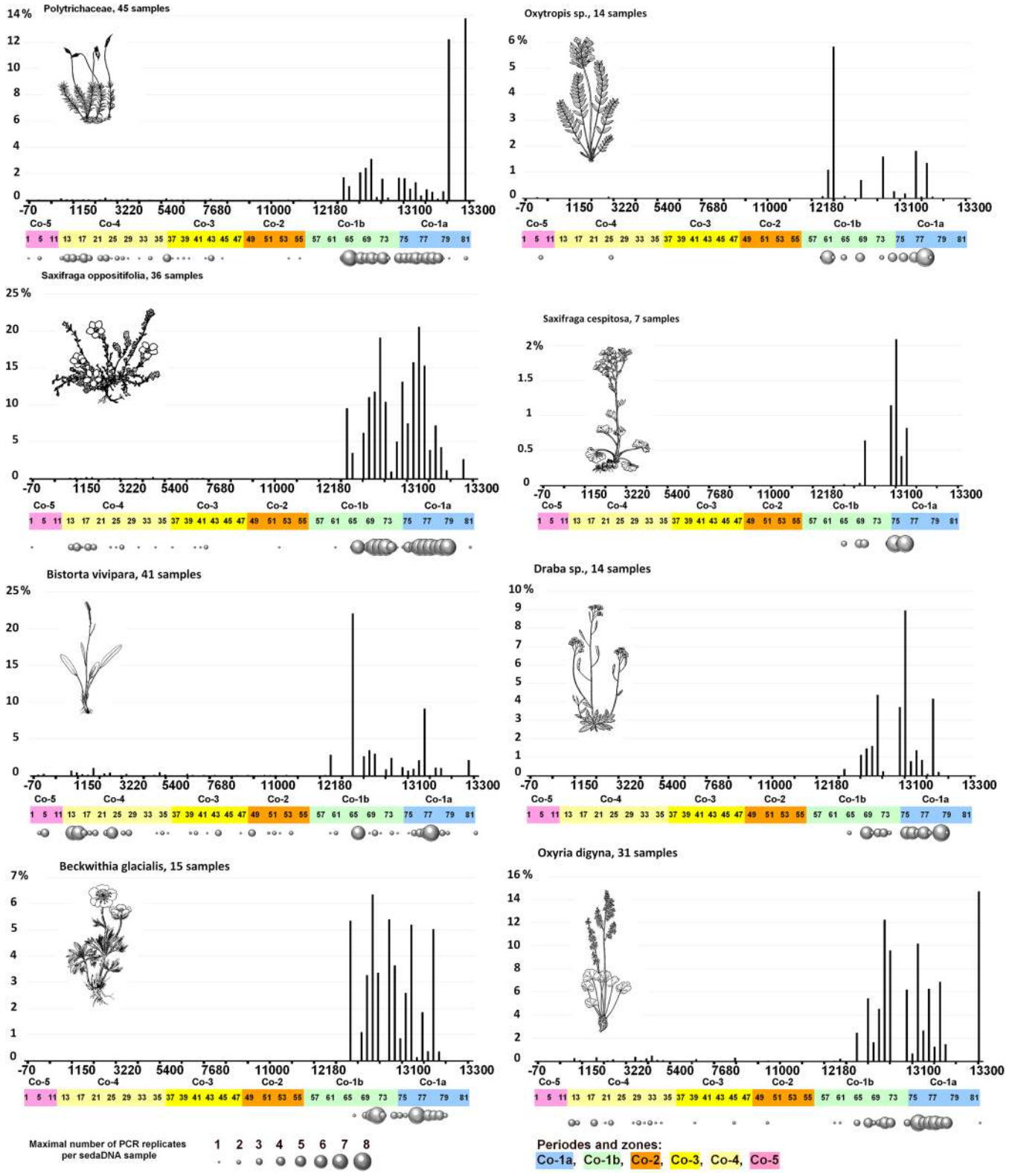



**Figure 8.** Occurrence of the most typical tundra and arctic–boreal plants over the past ca 13 300 a. Selected taxa functional groups are presented as a percentage of total *sed*aDNA reads per sample (histogram) and maximum number of PCR replicates (out of eight) per sample (round symbols below the X-axis) for the Lake Imandra palaeorecord. The X-axis describes age with associated palaeoecological zones below: samples are grouped in the following way. N1–12: Co-5 (Anthropogenic influence); N13–36: Co-4 (Late Holocene); N37–47: Co-3 (Mid Holocene); N48–56: Co-2 (Early Holocene); N57–73: Co-1b (Younger Dryas); N74–81: Co-1a (Allerød). The scale of Y-axis varies amongst panels. [Color figure can be viewed at wileyonlinelibrary.com]

Late Glacial Interstadial (i.e., Allerød warming that started presumably before our sediment record starts and is only represented in the sediment core Co1410 in a small part), with a gradual addition of new plant taxa over time. Regional patterns of the taxa accumulation are demonstrated in Figure 6. Thus, while it took millennia to build up the regional species pool, very few of the taxa that arrived are not found in the study area today.

This long, consistent, and taxonomically diverse reconstruction of the regional palaeofloras reveals most of the dominant and determinant plants that are characteristic of the present-day plant communities in the northern boreal forest (e.g., *Pinus*

© 2025 The Authors *Journal of Quaternary Science* Published by John Wiley & Sons Ltd. 

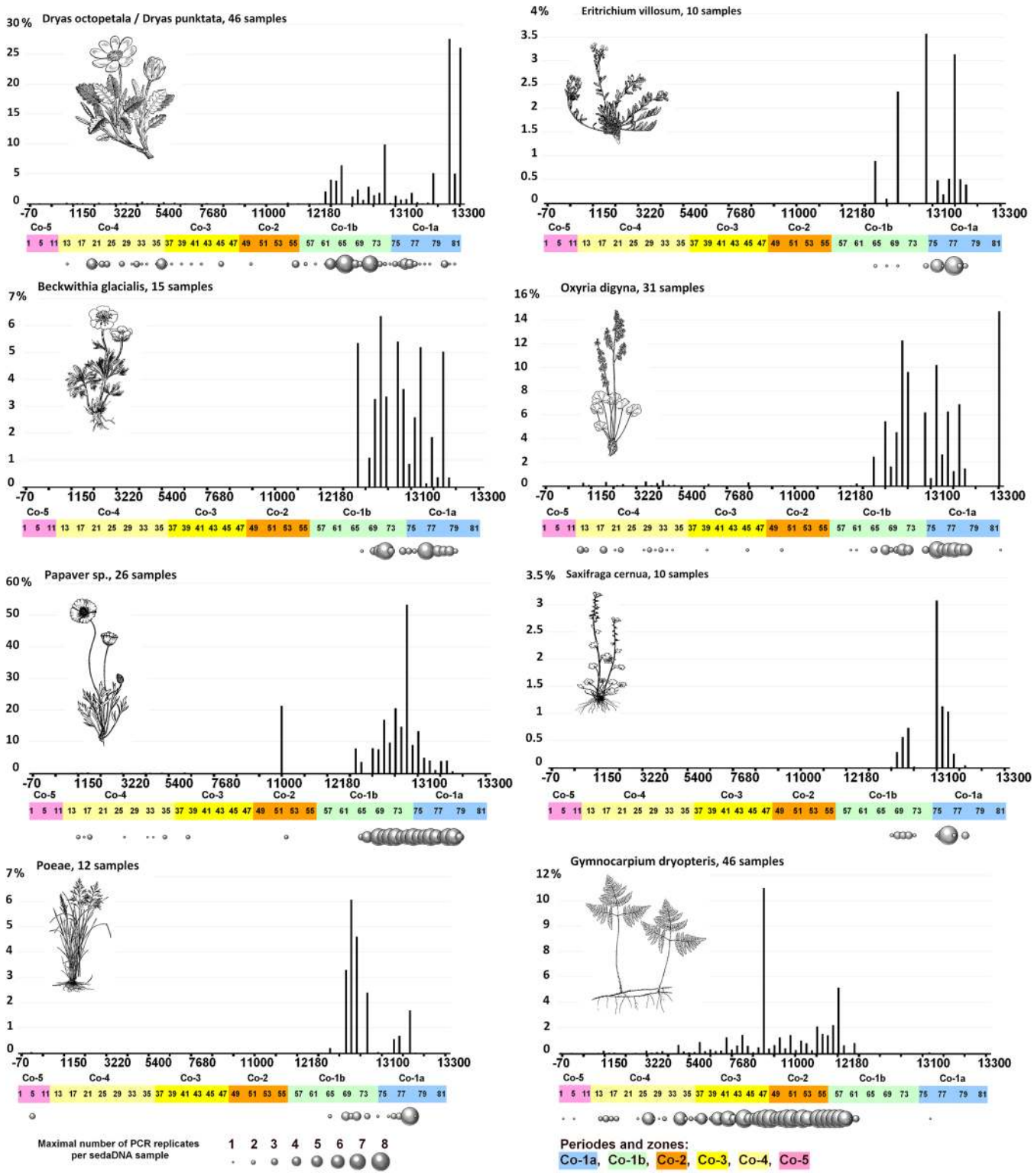



**Figure 9.** Occurrence of the most typical arctic–boreal and one boreal plant (*Gymnocarpium dryopteris*) over the past ca 13 300 a. Selected taxa functional groups are presented as a percentage of total *sed*aDNA reads per sample (histogram) and maximum number of PCR replicates (out of eight) per sample (round symbols below the X-axis) for the Lake Imandra palaeorecord. The X-axis describes age with chronological periods below: samples are grouped in the following way. N1–12: Co-5 (Anthropogenic influence); N13–36: Co-4 (Late Holocene); N37–47: Co-3 (Mid Holocene); N48–56: Co-2 (Early Holocene); N57–73: Co-1b (Younger Dryas); N74–81: Co-1a (Allerød). The scale of Y-axis varies amongst panels. [Color figure can be viewed at wileyonlinelibrary.com]

*sylvestris, Picea obovata, Betula* sp., *Alnus* sp., and *Salix* sp.). A number of typical admixture and understory taxa were identified to the level of species: for example, *Empetrum hermaphroditum Chamaepericlymenum suecicum, Melampyrum pretence, Geranium sylvaticum, Angelica archangelica, Trollius europaeus, Trientalis europaea*, as well as *Pyrola* and *Viola* species. Identification of Asteraceae, Orchidaceae, and many bryophytes taxa was limited by the method restrictions (especially for mosses, as our DNA extraction protocols are developed mainly for vascular plants, not for Bryophyta) and by the incomplete genomic reference database.

In addition, based on *sed*aDNA analysis, we were able to describe almost all (90%) of shrub tundra taxa with various ericoid dwarf shrubs and *Dryas*. We revealed up to 40% of

© 2025 The Authors *Journal of Quaternary Science* Published by John Wiley & Sons Ltd. 

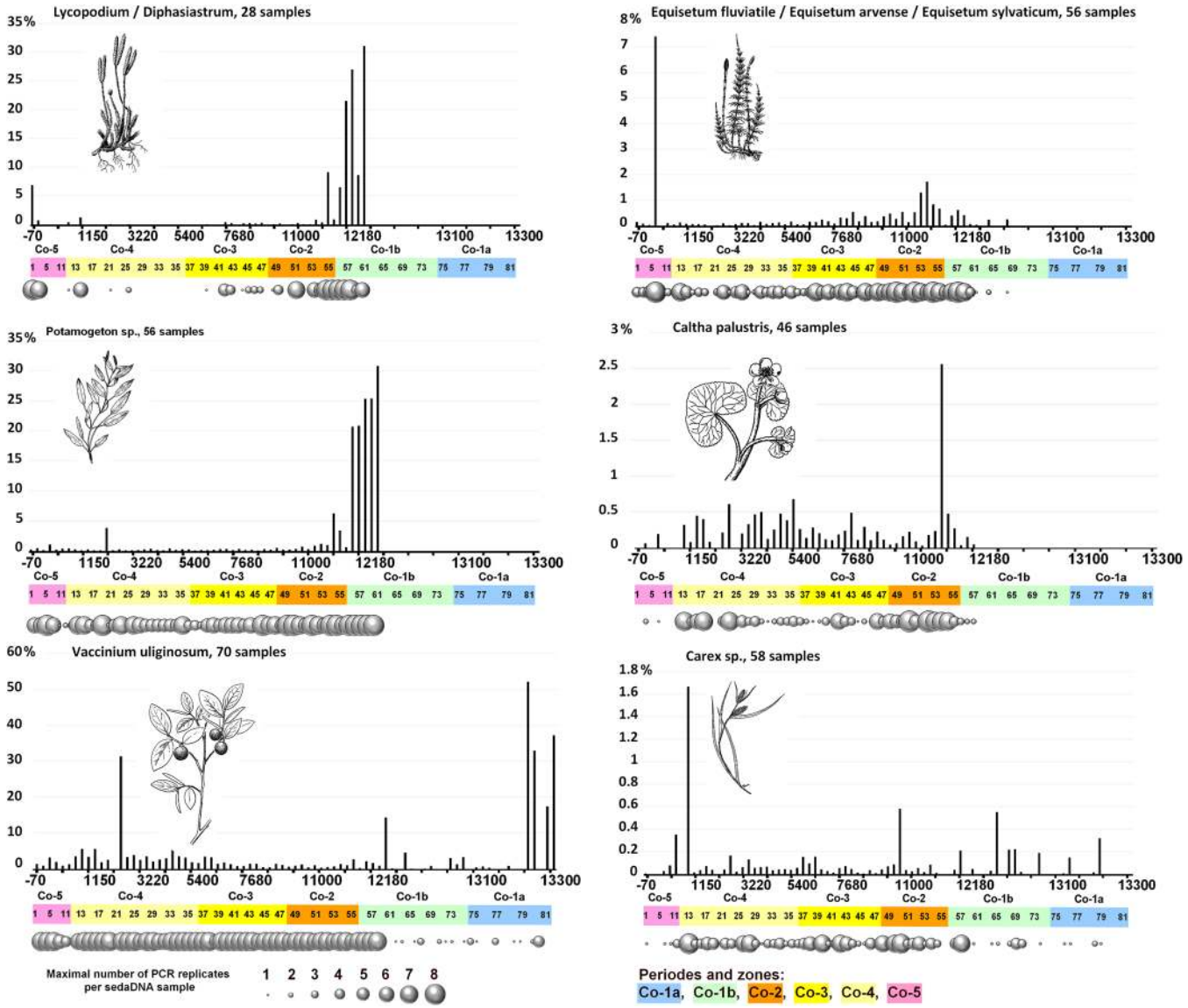



**Figure 10.** Occurrence of the most typical boreal and aquatic plants over the past ca 13 300 a. Selected taxa functional groups are presented as a percentage of total *sed*aDNA reads per sample (histogram) and maximum number of PCR replicates (out of eight) per sample (round symbols below the X-axis) for the Lake Imandra palaeorecord. The X-axis describes age with chronological periods below: samples are grouped in the following way. N1–12: Co-5 (Anthropogenic influence); N13–36: Co-4 (Late Holocene); N37–47: Co-3 (Mid Holocene); N48–56: Co-2 (Early Holocene); N57–73: Co-1b (Younger Dryas); N74–81: Co-1a (Allerød). The scale of Y-axis varies amongst panels. [Color figure can be viewed at wileyonlinelibrary.com]

the swamp taxa, including diverse species of *Carex, Eriophorum*, Juncaceae, Poaceae, Equesetaceae, and *Sphagnum*. Also, the number of identified ferns was rather high. Molecular methods allowed us to distinguish the most common fern on the Kola Peninsula (i.e., *Gymnocarpium dryopteris*) as well as *Dryopteris* sp. and some of the less common ones (e.g., *Phegopteris connectilis, Thelypteris palustris)*. Our data demonstrate that the last two species used to be much more common in the past (especially in the zone Co-2, Fig. 2) than at present.

Furthermore, the rare *Pteridium aquilinum* (Synonym: *Pteridium pinetorum* CAN. Page et R.R. Millwas) was identified. Nowadays this fern is very rarely encountered in the area (mainly in the dry forests and in the open birch woods in mountains) This fern is included into the Red Data book of Murmansk region (Rare plants and animals that need a protection in the Murmansk region, 1990; Konstantinova et al., 2003; Red Data Book of Murmansk Region. (2008) http://portal.kgilcaru/redbook/?q=redbookmainen) as a vulnerable species with decreasing population and a high risk of elimination. In the region, only three sites are known for this plant to occur: https://portal.kgilc.ru/redbook/?q=Pteridium_pinetorum). Its presence in the area is evidenced since at least the Early Holocene (zone Co-2, Fig. 2) with the maximum of occurrence at ca 11 000–8000 cal a BP and a strong decrease thereafter (Fig. 2).

As the lake Imandra is situated in the vicinity of the Khibiny Mountains (to the east of the lake; see Fig. 1(C)) with a mean altitude of 500–800 m and a maximal elevation of ca 1200 m, whose western slopes are drained into that lake, it is not a surprise that the sediments encountered a high proportion of tundra plants, such as *Astragalus* sp., *Beckwithia glacialis, Silene acaulis*, various *Saxifraga* species, *Oxyria digyna, Papaver* sp., with scattered occurrence even during modern time. Furthermore, about one third of aquatic and wetland plants known for the region nowadays were distinguished by the *sed*aDNA analysis, and 13 out of 23 aquatic taxa were identified up to the species level (see Supporting material S1, datasheet: List of taxa with assignments and S4: Phylogenetic relationship of identified taxa).

The high yields of *sed*aDNA and the diverse taxonomic spectra of identified plants are explained by the large, topographically and phytosociologically complex catchment area, the long temporal range of the core Co1014, and the high

© 2025 The Authors *Journal of Quaternary Science* Published by John Wiley & Sons Ltd. 

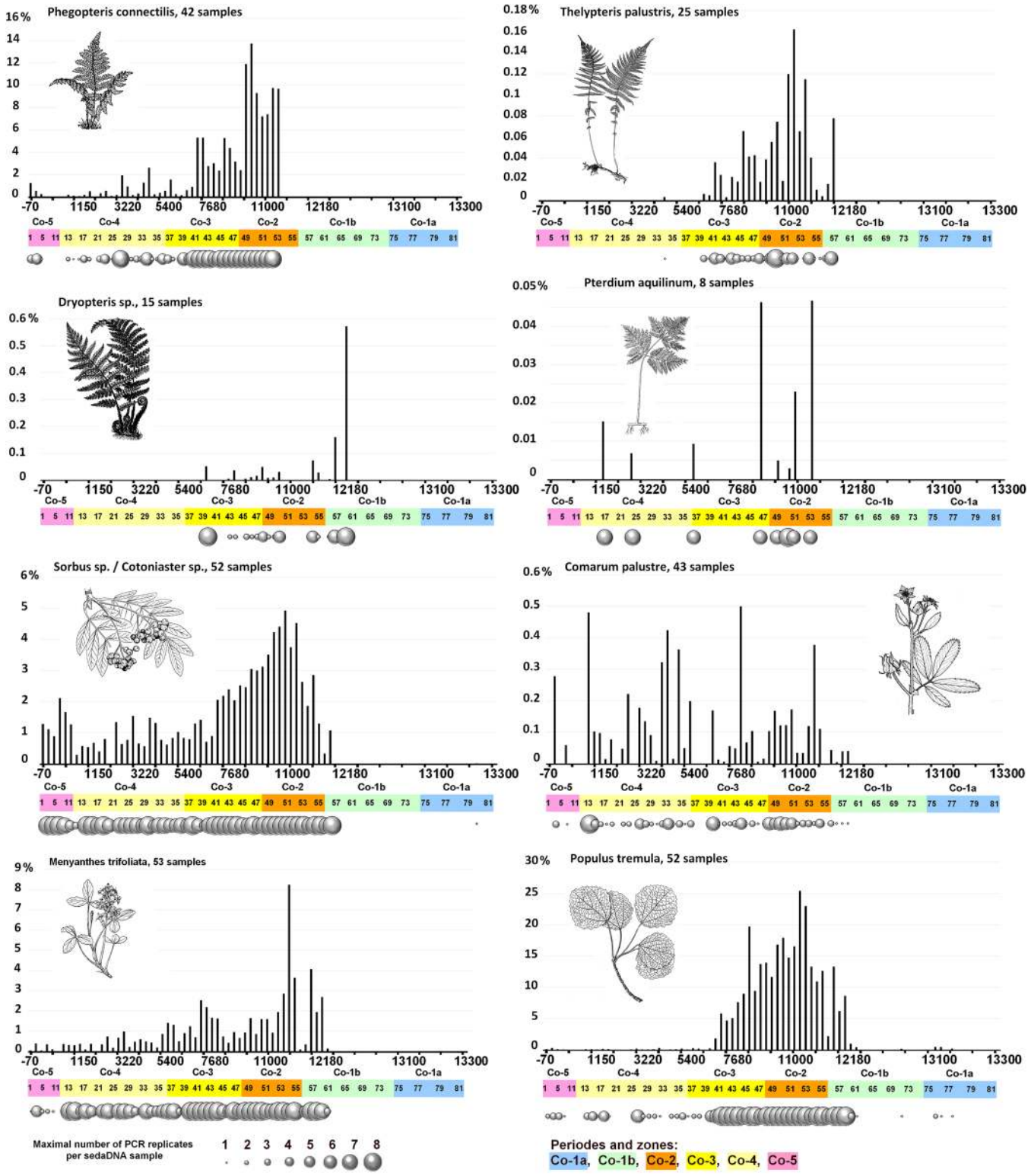



**Figure 11.** Occurrence of the most typical boreal plants over the past ca 13 300 a. Selected taxa functional groups are presented as a percentage of total *sed*aDNA reads per sample (histogram) and maximum number of PCR replicates (out of eight) per sample (round symbols below the X-axis) for the Lake Imandra palaeorecord. The X-axis describes age with chronological periods below: samples are grouped in the following way. N1–12: Co-5 (Anthropogenic influence); N13–36: Co-4 (Late Holocene); N37–47: Co-3 (Mid Holocene); N48–56: Co-2 (Early Holocene); N57–73: Co-1b (Younger Dryas); N74–81: Co-1a (Allerød). The scale of Y-axis varies amongst panels. [Color figure can be viewed at wileyonlinelibrary.com]

resolution of the applied analysis. Another reason may be the lithology, as the core predominantly consists of the fine-grained silty gyttia and clayey silt. These types of sediment allow better DNA preservation (Pietramellara et al., 2001; Cai et al., 2006; Huang, 2014; Pansu et al., 2015) compared to peat and gravel. Since *sed*aDNA has proved to identify a high number of taxa at a relatively good taxonomical resolution within different functional vegetation groups, the molecular methods employed on core Co1410 have a high potential for palaeoecological investigations with unprecedented accuracy. Along with the high sample number and the detailed age-depth model of the record, a unique insight into the environmental and vegetation change in the central Kola Peninsula for the last ca 13 300 cal a BP is gained.

© 2025 The Authors *Journal of Quaternary Science* Published by John Wiley & Sons Ltd. 

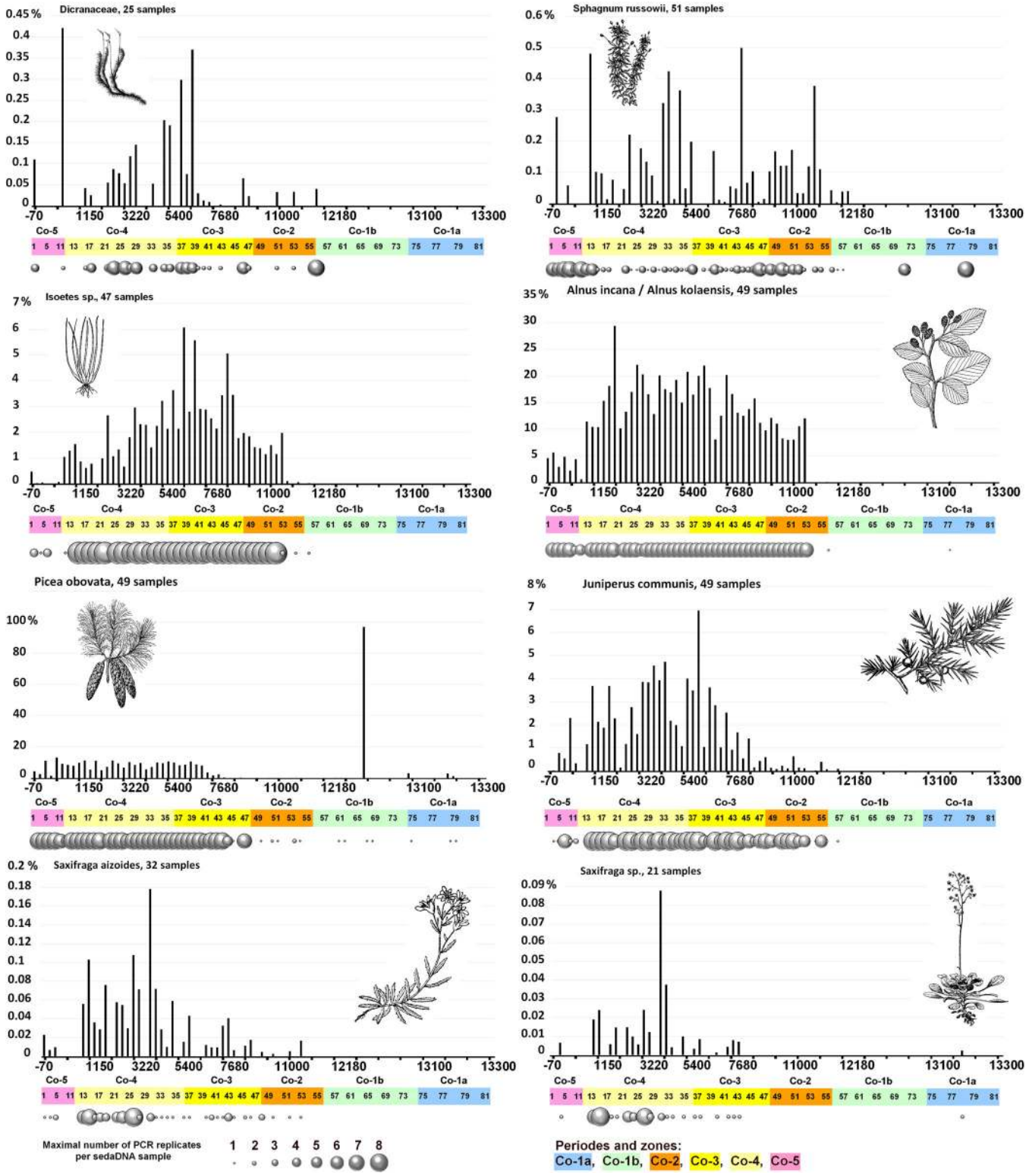



**Figure 12.** Occurrence of the most typical boreal and boreal–nemoral plants over the past ca 13 300 a. Selected taxa functional groups are presented as a percentage of total *sed*aDNA reads per sample (histogram) and maximum number of PCR replicates (out of eight) per sample (round symbols below the X-axis) for the Lake Imandra palaeorecord. The X-axis describes age with chronological periods below: samples are grouped in the following way. N1–12: Co-5 (Anthropogenic influence); N13–36: Co-4 (Late Holocene); N37–47: Co-3 (Mid Holocene); N48–56: Co-2 (Early Holocene); N57–73: Co-1b (Younger Dryas); N74–81: Co-1a (Allerød). The scale of Y-axis varies amongst panels. [Color figure can be viewed at wileyonlinelibrary.com]

## *History of vegetation and local environment*

### *ca 13 300–13 000 cal a BP (Allerød, Zone Co-1a)*

Subzone Co-1a, formed between ca 13 000–13 300 cal a BP, is attributed to Allerød warming (e.g., Merkt, 1994; Björck et al., 1998; Litt and Stebich, 1999; Merkt and Müller, 1999, Rasmussen et al., 2006; Hättestrand et al., 2008; Kolka et al., 2008; Nogarotto et al., 2023; Thiagarajan et al., 2014; Fig. 7), sometime after the initial deglaciation. So far, no sediment material retrieved from the region was unambiguously dated back to the time of the initial deglaciation (Solovieva and Jones, 2002; Solovieva et al., 2005; Olyunina et al., 2008; Ilyashuk et al., 2013; Tolstobrova et al., 2016; Shilova et al., 2019; Lenz et al., 2020). Studies on core

© 2025 The Authors *Journal of Quaternary Science* Published by John Wiley & Sons Ltd. 

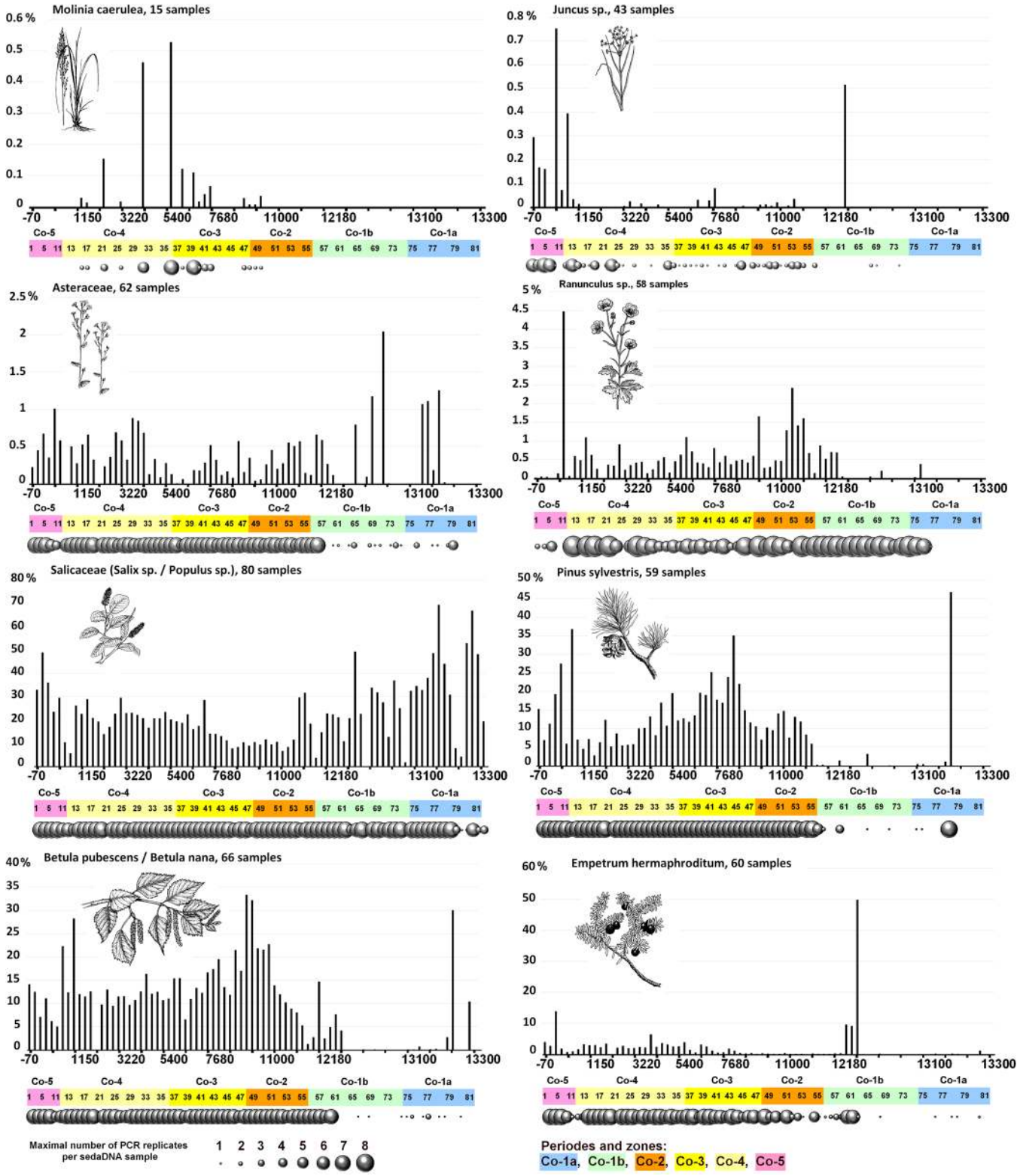



**Figure 13.** Occurrence of some multizonal plants over the past ca 13 300 a BP. Selected taxa functional groups are presented as a percentage of total *sed*aDNA reads per sample (histogram) and maximum number of PCR replicates (out of eight) per sample (round symbols below the X-axis) for the Lake Imandra palaeorecord. The X-axis describes age with chronological periods below: samples are grouped in the following way. N1–12: Co-5 (Anthropogenic influence); N13–36: Co-4 (Late Holocene); N37–47: Co-3 (Mid Holocene); N48–56: Co-2 (Early Holocene); N57–73: Co-1b (Younger Dryas); N74–81: Co-1a (Allerød). The scale of the Y-axis varies among panels. [Color figure can be viewed at wileyonlinelibrary.com]

Co1410, involving litho- and biostratigraphy (Lenz et al., 2020) and molecular methods (this study) suggest that deglaciation commenced some time before 13 300 cal a BP. An age older than that at the core base is expected since some taxa that are constantly present in the record were detected (Fig. 3(A): Shrubs and dwarf shrubs), and any vegetation needs time to develop. The development of initial vegetation was probably triggered by the warming following the preceding glacial conditions, as suggested by a simultaneous increase in local July temperatures, as it was reconstructed by Ilyashuk et al. (2013) based on the aquatic invertebrates (i.e., chironomids, ceratopogonids, and exoskeletons of aquatic oribatids) from the Lake Kupal'noe in the central part of the Khibiny mountains, and supported by the increase of annual temperatures in central

© 2025 The Authors *Journal of Quaternary Science* Published by John Wiley & Sons Ltd. 

Greenland, suggested by $d^{18}O$ data from the GISP2 ice core (Cuffey and Clow, 1997; Alley, 2000) (Fig. 7(A)).

In this subzone, dwarf-shrub dominated open communities occurred, with Salicaceae shrubs, some participation of *Betula* (*B. nana* apparently), *Dryas octopetala/Dryas punktata,* and *Empetrum hermaphroditum*. These are cold- and wind-tolerant taxa, which today occur in the mountains at elevations of 400 m and higher (personal observation). Both the new *sed*aDNA data and previously published pollen data derived from the core Co1410 (Lenz et al., 2020) reflect that not many forbs and graminoids were included in the initial plant communities. This confirms cold but already partly ice-free conditions, which agree with the reconstruction of the ice sheet and mountain glaciations in the Khibiny Mountains to the southeast of the coring site by Yevzerov and Nikolaeva (2008). To add more, our findings obtain support in the earlier, both regional (Kremenetski et al., 2004) and super-regional reconstructions (Velichko et al., 2017), which suggest that the Lateglacial vegetation of the Kola Peninsula was dominated by shrub tundra with *Betula nana*, *Salix* sp., and characterised by the presence of the typical pollen indicators of cold climates, namely *Saxifraga* sp., *Dryas* sp., and *Ephedra* sp. Although the last genus is not revealed in our *sed*aDNA record, similar pollen assemblages pointing to the occurrence of tundra–steppe formations are known for this period from northernmost Fennoscandia (Hyvärinen, 1976; Prentice, 1982; Seppä, 1996).

### *ca 13 000–11 800 cal a BP (Younger Dryas, Zone Co-1b)*

The palaeoecological zone Co-1b was formed during ca 13 000–11 800 cal a BP and mainly corresponded to the Younger Dryas chronozone (Andersen et al., 1995; Mangerud et al., 2011; Stroeven et al., 2016; Patton et al., 2017; Boyes et al., 2021), when relatively cool climatic conditions are reported (Lohne et al., 2013).

Steppe–tundra, rather poor in shrubs but more diverse in forbs and graminoids (Figs. 2(D) and 7), occurred in the study area in this time zone. Typical tundra cold-tolerant taxa (e.g., *Oxygraphis glacialis, Saxifraga oppositifolia* and *S. cespitosa, Bistorta vivipara, Draba* sp., *Beckwithia glacialis, Oxyria digyna*, as well as mosses from the Polytrichaceae family expanded in the area, as it is suggested by molecular methods (Figs. 8 and 9), and DCA (Fig. 5(B)) supported this statistically. After ca 12 180 a BP, *Andromeda polifolia, Chamaedaphne calyculata, Phyllodoce caerulea*, diverse Asteraceae and *Micrantes* species, *Eriophorum villosum*, and *Papaver* sp. occurred synchronously (Figs. 2, 4(B), 8, and 9). Arboreal vegetation is unlikely to have developed during this period, and, despite a prominent increase in the number of identified taxa, findings of *Pinus sylvestris, Picea obovata,* and *Populus tremula* during the Younger Dryas in *sed*aDNA should be treated with caution. Cold and relatively dry climate conditions are not favourable for the development of the forests, and the previous reconstructions of the regional vegetation suggest that more open communities consisted of a shrub birch-willow tundra prevailed (Kremenetski et al., 2004). Velichko et al. (2017) also suggest an open dwarf shrub–moss tundra in the central part of the Kola Peninsula for the Younger Dryas. The abundance of graminoid was the highest during this period (Fig. 7(A)) for the entire record. This stays in agreement with the suggested by *sed*aDNA analyses open plant communities in the area and finds a good support in the regional literature (Nikonov and Vostrukhina, 1964; Nikonov, 1966; Solovieva and Jones, 2002; Krikunova et al., 2022).

As *sed*aDNA analyses may work not well enough with Asteraceae family (Nichols et al., 2018), the boreal Asteraceae attributed to *Cirsium* (Fig. 2(B) Forbs_Beginning) is likely done erroneously: no typical environment for these taxa could be described in this period, and other plants phytosociologically associated with those taxa are missing in the record as well. Furthermore, *Cirsium* species are rather highly demanding of the soil trophic conditions, and it is unlikely that suitable soils would have developed in tundra at the discussed times. Instead, cold-tolerant Asteraceae occurring in the modern wet tundra could present, for example, *Artemisia* sp., *Solidago* sp., *Saussurea* sp. Asteraceae pollen is often found in the various study sites of the region (e.g., Kremenetski et al., 1999; Krikunova et al., 2022); however, in the absence of detailed morphological studies on pollen and evidence from scanning electron microscopy, we have neither support nor contradictions for our assumptions on Asteraceae. Increased amounts of shrubs and forbs in this zone may be related not only to the overall increasing air temperature and glacier ice retreat, but probably also to the occurrence of the water streams along the meltwater channels (Whittaker, 1993).

### *ca 11 800–8500 cal a BP (Early Holocene, Zone Co-2)*

The palaeoecological zone Co-2 is dated between ca 11 800 and 8500 cal a BP. This period experienced slightly warmer conditions and reasonably long summer periods without lake ice, as some hydrophilic, aquatic taxa (e.g., *Pogonatum* moss species, *Caltha palustris, Comarum palustre, Menyanthes trifoliata*, Figs. 10 and 11) and algae increased in their abundances. Notably higher diversity and marked abundances of these insect-pollinated plants could only have an opportunity to develop if the warmer conditions during the vegetation season occur as it is suggested in the palaeobotanical investigations from the Scandinavian mountains, which show that the Early Holocene in Fennoscandia had summer temperatures of at least 1°C–1.3°C higher than today at ca 9500–8000 cal a BP (Kullman, 2002; Paus and Haugland, 2017).

The plant *sed*aDNA data suggest the occurrence of open grasslands gradually changing to a mixture of woody (mainly birch) and forb/grass dominated communities (Fig. 2(A): Trees and Shrubs and Fig. 7(B)). Environmental conditions were apparently wetter than in the previous period, as *Equisetum* species, *Lycopodium* sp./*Diphasiastrum* sp., and some ferns increased their abundances. From about 11 200 cal a BP trees and high woody shrubs (i.e., birch, pine, juniper, and alder) were constantly present in the regional vegetation (Figs. 7(B) and 10), which is markedly earlier than it was previously suggested, for example, by Kremenetski et al. (2004) who evidenced the early Holocene birch forest expansion across the Kola Peninsula at ca. 9500 cal a BP. Snyder et al. (2000) also refers to the early Holocene birch period in the Kola Peninsula.

Modern palynological findings point to the increasing moisture levels and spread of pine already in the Early Holocene, starting as early as ca. 9300 cal a BP (Krikunova et al., 2022). These reconstructions point to the increased glacial meltwater supply during this time (e.g., as described by Kalugin et al.; Kylander et al., 2011) as well as the increases in *Artemisia* sp. pollen and the total pollen concentrations that Lenz et al. (2020) interpret as "more favourable growing conditions for the vegetation in the catchment." Our *sed*aDNA data stay in agreement with these findings.

### *ca 8500–5500 cal a BP (Zone Co-3)*

Zone Co-3 was formed between ca 8500–5500 cal a BP and represents most of the Middle Holocene. This period at the Lake Imandra was characterised by a strong increase in plant diversity, reflected in higher taxa number (141 vs. 109 in the previous zone, Table 1 and Figs. 4, 7, and 10). Besides, notable changes in the vegetation composition occurred. For

© 2025 The Authors *Journal of Quaternary Science* Published by John Wiley & Sons Ltd. 

instance, trees played an increased role in the vegetation, and forbs became a prominent feature. In addition, ferns and aquatic plants reached a high diversity (Figs. 2(A),(D) and 10), a number of relatively thermophilic plants occurred, for example, *Lonicera* species, *Populus tremula, Sorbus* sp./*Cotoneaster* sp. All ericoid dwarfs, modernly known for the central Kola Peninsula, were present in this period. This corresponds to the regional Mid-Holocene Thermal Maximum as Vaschalova and Klimanov (1987) evidenced it at ca 6000–5000 a BP, and Krikunova et al. (2022) found it in the maximum pollen percentages during ca 8200–4200 cal BP. Comparable evidence was also obtained for Northern Norway (Alm et al., 1996), for Finland (Väliranta et al., 2015), and for Sweden, where the Mid-Holocene Thermal Maximum occurred between ca 8000 and 5000 a BP (Wastegård, 2022).

Higher annual and summer temperatures in the study area after ca 7700 cal a BP are well supported by the constant presence of *Nuphar* sp./*Nymphaea* sp. (Fig. 2(A)) amongst the aquatic plants. *Nymphaea* species are highly sensitive to cold conditions. Two species of this genus (i.e., *Nymphaea candida* J. Presl and *Nymphaea tetragona* Georgi) are mentioned in the flora of the Murmansk Region (https://www.murman.ru/flora/data/l000018.shtml), but to our knowledge, nowadays they are not known for the lake Imandra at all. *Nuphar* sp. is very rarely encountered in Imandra. Three species (i.e., *Nuphar lutea* (L.) Smith, *Nuphar pumila* (Timm) DC, and *Nuphar x spenneriana* Gaudin) are mentioned for the Kola Peninsula, mainly for its southern part. Two of the mentioned plants are included in the Red Data Book of the Murmansk Region: *Nymphaea candida* J. Presl as the vulnerable species with decreasing population (https://portal.kgilc.ru/redbook/?q=Nymphaea_candida) and *Nymphaea tetragona* Georgi as the critically endangered species under the immediate threat of elimination (https://portal.kgilc.ru/redbook/?q=Nymphaea_tetragona). *Nuphar lutea, N. pumila, Nymphaea candida,* and *N. tetragona* are also included in the European Red List of Vascular Plants (Bilz et al., 2011). Our study suggests that for the study area, rare plants decreased their abundances after ca 3500 cal a BP, most likely due to the overall cooling (Seppä et al., 2009; Krikunova et al., 2022).

Comparison of the *sed*aDNA abundances of *Betula* sp. and *Pinus sylvestris* suggests that the dominant vegetation type in this period was deciduous forest, which consisted of *Betula* sp. (*B. pubescens* is the most common in the area nowadays) with some admixture of pine, rich understory, and diverse forbs. This appears to contradict the reconstructions by Kremenetski et al. (1999) and MacDonald et al. (2000), and may possibly reflect some specific microregional vegetation dynamics in the Imandra catchment. After 7600 cal a BP (Fig. 12) spruce was constantly present in the vegetation but did not yet play a significant role. Its presence was from ca 6000 cal a BP, apparently scattered as suggested by Krikunova et al. (2022). In general, this assumption on the fragmented and irregular spruce spreading does not contradict to the earlier reconstructions of Kremenetski et al. (1999) stating that *Picea obovata* got widespread in the Kola Peninsula between ca 7000 and 5000 a BP, but we can point out that its expansion could have started in the catchment of the lake Imandra some 2000 year earlier. Absence of competition from pine could have played a role in that.

Most abundant were boreal and boreal–nemoral taxa, such as *Frangula alnus* (according to our own observations, it occurs seldom in nature at present, and is almost only known from the gardens), *Prunus padus* (common today in the lowlands and submountain forests but not abundant), *Prunella vulgaris, Thalictrum* sp., *Trientalis europaea, Viola* sp., *Sparganium* sp., and all ferns. Moreover, *Lonicera* species plays a rather high role (Fig. 2(A)). The last is surprising, taking into account that nowadays *Lonicera* × *subarctica Pojark*. is the only species from this genus known in the native flora of the Murmansk region; it occurs only sporadically along the rivers and water streams in the lowlands. All these findings suggest rather humid climate conditions during this period (Fig. 7), especially during the regional Mid-Holocene Thermal Maximum.

### *ca 5500–520 cal a BP (Zone Co-4)*

Zone Co-4 was formed between ca 5500–520 cal a BP. According to the *sed*aDNA record, this period is characterised by mixed coniferous/deciduous forest with an increased role of pine (Fig. 13) and especially spruce (Fig. 12) in the vegetation. The number of plant taxa registered is the highest (177, Table 1). The lack of statistically significant dynamics in the overall taxa composition indicates that the environmental conditions during this period were relatively stable. Reconstructions by Solovieva and Jones (2002) from the Chuna Lake (central part of the Kola Peninsula) also indicate that during the past ca 4200 years, their diatom record did not reveal any clear response to environmental changes. That contrasts with the pollen records from Northern Europe, where a lot of dynamics is suggested during this period (e.g., Wastegård, 2022). A continuous cooling trend with some pronounced cold events was identified (Seppä et al., 2009), but we did not observe any regionally important events alike. An exception in our record is the period of ca 4000–3200 a BP, which corresponds to the beginning of the Subboreal period (Figs. 4 and 7), when a decrease in taxa diversity occurred most likely because of the colder conditions. A simultaneous decrease in ferns suggests either drier regional conditions or the loss of their typical habitats.

### *Ca 520– -70 cal a BP (The latest time, Zone Co-5)*

Zone Co-5 reflects the past ca 500 years, when the lake Imandra was heavily influenced by the industrial and agricultural activities, especially after the 1930s (Moiseenko and Yakovlev, 1990; Moiseenko et al., 2009). Reconstructed vegetation in this time interval is characterised by mixed coniferous forest with some presence of birch and dwarf shrubs (Figs. 2 and 7) that well describes general patterns of the present-day local vegetation communities. Common components of the modern flora are detected, that is, Asteraceae, *Empetrum hermaphroditum, Juncus* sp., *Ranunculus* sp., Salicaceae and *Pinus sylvestris* (Fig. 13). The topmost samples, which relate to the time after ca 250 cal a BP (1700 CE), are notably different from all others in the record, as they contain a number of plant taxa used for food and/or as medicinal and ornamental plants: that is, *Ribes* sp., which is popular for growing in the gardens, as well as *Hypericum* sp. and *Mentha arvensis*. Further indication of the human activity comes from the eutrophic taxa, namely *Trifolium* sp. and *Urtica dioica*. These plants are not known from the natural regional flora (e.g., Gorodkov, 1953), nor are they seen in the record during the warmest time of the Mid-Holocene. We assume that most likely these plants were brought into the study area with the spread of agriculture, hay harvesting, and the use of fertilisers, as the time of their chronologically first occurrence corresponds with the regional population increase (Moiseenko et al., 2009) and rapid economic development of the Murmansk region.

## Summary and conclusions

Sediment core Co1410 from Lake Imandra, deposited since approximately 13 300 cal a BP, was investigated using molecular methods, that is, *sed*aDNA analysis and metabarcoding. The results provide unprecedented detail on postglacial vegetation

© 2025 The Authors *Journal of Quaternary Science* Published by John Wiley & Sons Ltd. 

and environmental patterns in the western Kola Peninsula. Based on them, the following conclusions can be drawn:

(1) The record well reflects the already known regional stratigraphy. It begins from the Late Pleistocene warming phase (Allerød, ca 13 300–13 000 a BP, Co-1), apparently slightly after the glacial retreat and initial colonisation of the ground by primary tundra vegetation.
(2) Zone Co-2 corresponds to the Younger Dryas and describes a cold period characterised by a transition from tundra with dwarf shrubs to more open grasslands with forbs, along with the re-advance of the glaciers in the catchment of the Grater (Bolshaya) Imandra area around ca 13 000–11 800 cal a BP.
(3) In the zone Co-3, from ca 11 800 to 8500 cal a BP, relative warming led to increased plant diversity with the formation of open grasslands, followed by the establishment of birch forests.
(4) Zone Co-4 occurred at ca 8500–5500 cal a BP. It is characterised by the highest regional plant diversity (177), establishment of deciduous/coniferous woody vegetation established in the research area during this period, woody vegetation in the form of a mosaic of mixed coniferous and deciduous forest, and a high contribution of thermophilic plant taxa (i.e., *Lonicera species, Populus tremula, Sorbus/Cotoneaster* sp.), aquatic plants and ferns, including the rare for the Murmansk region *Pteridium aquilinum* and *Nuphar* sp./*Nymphaea* sp. those highest occurrence of which revealed in *sed*aDNA corresponded to the Mid-Holocene Thermal Maximum.
(5) During the last palaeovegetation zone Co-5 between ca 5500 and −70 cal a BP, modern vegetation communities established. In recent times (from around ca −62 to ca −70 cal a BP), a slight increase in biodiversity is noticed, traced to the increased presence of cultural plants and weeds.
(6) Studies on the regional plant taxonomic spectra from ca 13 300 a BP to the present time revealed a high proportion (97%) of taxa known from the present-day flora. This demonstrated that the regional pool of taxa, except rare and mostly thermophilic species, formed already as early as the Allerød.

*Acknowledgements.* The authors acknowledge the cooperation, experience, and assistance of the colleagues from the Geological Institute of the Kola Science Centre of the Russian Academy of Sciences (GI KSC RAS) in Apatity during the coring campaign in summer 2017. Dr. Arve Elvebak (UiT Museum, Tromsø) gets our gratitude for his help in our identification of the bryophytes and for a critical revision of the taxa checklists. Youri Lammers and Sandra Garces Pastor are acknowledged for their assistance in bioinformatics and discussions during the preparation of the manuscript; Sandra is also thanked for the DNA library preparation and quantification. The first author thanks the Regional Editor of the *Journal of Quaternary Science,* Prof. Achim Bauer, and two anonymous reviewers for their comments and help to improve the draft of the manuscript. Financial support for this study was provided by the Research Council of Norway (grant number 296987/E50), by the German Research Foundation (DFG—grant no ME 1169/28), and by the German Federal Ministry of Education and Research (BMBF—grant no. 03G0859A). This study has been carried out within the international multidisciplinary programme Future ArcTic Ecosystems (FATE): drivers of diversity and future scenarios from ethnoecology, contemporary ecology, and ancient DNA (https://www.fate-biodivscen.org). The article contributes to the FATE network. Open Access funding enabled and organized by Projekt DEAL.

## *Data Availability Statement*

Poliakova, A., Lenz, M., Melles, M., Fedorov, G.B; Alsos, I.G. Data on the chronology of the sediment core Co1410 (Lake Imandra, NW Russia, Murmansk Region): 14C dates and tie points, *sed*aDNA weighted PCR repeats, *sed*aDNA total reads, and biogeochemical data: PANGAEA, https://doi.pangaea.de/10.1594/PANGAEA.942504

Poliakova, A; Lenz, M; Melles, M et al.: Table of taxa names and their assignments to families, growth form, geographical distribution group of sediment core Co1410: PANGAEA, https://doi.pangaea.de/10.1594/PANGAEA.942491

Poliakova, A; Lenz, M; Melles, M et al.: Sediment ancient DNA total reads of sediment core Co1410. PANGAEA, https://doi.pangaea.de/10.1594/PANGAEA.942501

Poliakova, A; Lenz, M; Melles, M et al.: Sediment ancient DNA weighted PCR repeats of sediment core Co1410. PANGAEA, https://doi.pangaea.de/10.1594/PANGAEA.942493

The *sed*aDNA sequence data have been deposited in the European Nucleotide Archive (ENA) (www.ebi.ac.uk/ena/browser/home) with BioProject accession PRJEB71946.

## Supporting information

Additional supporting information can be found in the online version of this article.

**S1:** All taxa identified in metabarcoding of *sed*aDNA from Lake Imandra (Kola Peninsula (NW Russia), after sequence filtering. Names in brackets represent known local/regional species resulting from sequence match in reference libraries or BLAST results, in case no species were identified in reference libraries.

**S2:** Age-depth model of the sediment profile Co1410, based on six $^{14}$C ages derived from organic macro-remains and additional tie points from 137Cs and Hg measurements as well as pollen stratigraphy with the upper and lower boundary of the Younger Dryas according to Lohne et al. (2013) for northern Europe. The sedimentation rate displayed on the right was calculated from the Bayesian age-depth model. The upper bar shows the stratigraphical framework of the study. Al = Allerød; YD = Younger Dryas; EH = Early Holocene; MH = Middle Holocene; LH = Late Holocene; A = anthropogenic influence. The black rectangle in the bar at the bottom indicates the period not reflected by the core as a result of a core gap between 6.92 and 7.54 m. Modified after Lenz et al., 2020. For details, see the Results and Discussion below.

**S3:** Phylogenetic relationship of identified taxa.

**S4:** Complete results of DCR analysis.

**S5:** Models and reconstruction of the ice margin positions in the Late Glacial and thereafter. Scheme is modified after the Database on the Palaeoclimate and sea level changes in the Arctic and Antarctic (AARI, 2010) and modern studies (See References).

*Abbreviations.* bp, base pair; BP, before present; ca, circa; cal, calibrated; CE, common era; DCA, detrended correspondence; Fig., Figure; P, probability; PCR, polymerase chain reaction; SD, standard deviation; SedaDNA, sedimentary ancient DNA; sp., species analysis.

## References

Aario, L. (1943) Über die Wald- und Klimaentwicklung an der lappländischen Eismeerkuste in Petsamo, mit einem Beitrag zur nord und mittel europäischer Klimageschichte. *Annales Botanici Societatis Zoologica Botanica Fennicae 'Vanamo'*, 19(1), 1–158. [In German].

Alley, R.B. (2000) Ice-core evidence of abrupt climate changes. *Proceedings of the National Academy of Sciences*, 97, 1331–1334.

Alm, T., Vorren, K.-D. & Morkved, B. (1996) Holocene tree-line fluctuations and climate in central Troms, Northern Norway. *Historical Biology*, 12, 25–38.

Alsos, I.G., Rijal, D.P., Ehrich, D., Karger, D.N., Yoccoz, N.G., Heintzman, P.D. et al. (2022) Postglacial species arrival and diversity buildup of northern ecosystems took millennia. *Science Advances*, 8, eabo7434.

© 2025 The Authors *Journal of Quaternary Science* Published by John Wiley & Sons Ltd. 

Alsos, I.G., Sjögren, P., Brown, A.G., Gielly, L., Merkel, M.K.F., Paus, A. et al. (2020) Last Glacial Maximum environmental conditions at Andøya, northern Norway; evidence for a northern ice-edge ecological 'hotspot'. *Quaternary Science Reviews*, 239, 106364. Available from: https://doi.org/10.1016/j.quascirev.2020.106364

Alsos, I.G., Sjögren, P., Edwards, M.E., Landvik, J.Y., Gielly, L., Forwick, M. et al. (2016) Sedimentary ancient DNA from Lake Skartjørna, Svalbard: assessing the resilience of arctic flora to Holocene climate change. *The Holocene*, 26, 627–642. Available from: https://doi.org/10.1177/0959683615612563

Andersen, B.G., Lundqvist, J. & Saarnisto, M. (1995) The younger Dryas margin of the scandinavian ice sheet—an introduction. *Quaternary International*, 28, 145–146. Available from: https://doi.org/10.1016/1040-6182(95)00043-i

Anisimov, M.A. & Moskalenko, I.G. (2006) Usloviya retsentnykh i subretsentnykh sporovo-pyl'tsevykh spektrov na o-ve Bennetta (Novosibirskiye ostrova). *Vestnik Sankt-Peterburgskogo Gosudarstvennogo universiteta. Ser.* 7(1), 130–138. [in Russian].

Armand, A.D. & Samsonova, L.Y.a (1969) Marine sediments and Holocene tectonics of the Kandalaksha region, in: Major Problems of the Anthropogene Geomorphology and Stratigraphy of the Kola Peninsula. *Nauka, Leningrad*, 96, 111. [in Russian].

Bernardová, A. & Košnar, J. (2012) What do Holocene sediments in Petuniabukta, Spitsbergen reveal? *Polish Polar Research*, 33, 329–345. Available from: https://doi.org/10.2478/v10183-012-0023-2

Bilz, M., Kell, S.P., Maxted, N. & Lansdown, R.V. (2011) *European red list of vascular plants*. Luxembourg: Publications Office of the European Union.

Björck, S., Walker, M.J.C., Cwynar, L.C., Johnsen, S., Knudsen, K.L., Lowe, J.J. et al. (1998) An event stratigraphy for the Last Termination in the north Atlantic region based on the Greenland ice core record: a proposal by the INTIMATE group. *Journal of Quaternary Science*, 13, 283–292.

Bjune, A.E., Alsos, I.G., Brendryen, J., Edwards, M.E., Haflidason, H. & Johansen, M.S. et al. (2021) Rapid climate changes during the Lateglacial and the early Holocene as seen from plant community dynamics in the Polar Urals, Russia. *Journal of Quaternary Science*, 37, 805–817.

Bjune, A.E., Mangerud, J. & Moe, D. (2005) Past grazing habitats for Svalbard reindeer indicated by the pollen content of 3300-year-old faeces from Edgeøya, Svalbard. *Grana*, 44, 45–50. Available from: https://doi.org/10.1080/00173130410005564

Blaauw, M. & Christen, J.A. (2011) Flexible paleoclimate age-depth models using an autoregressive gamma process. *Bayesian Analysis*, 6, 457–474.

Blaauw, M., Christen, J.A., Aquino Lopez, M.A., Vazquez, J.E., Gonzalez, O.M. & Belding, T. et al. (2020) *Package 'rbacon'—age-depth modelling using Bayesian statistics*. Belfast: Queen's University Belfast.

Boulton, G. (2001) Palaeoglaciology of an ice sheet through a glacial cycle: the European ice sheet through the Weichselian. *Quaternary Science Reviews*, 20, 591–625.

Boyer, F., Mercier, C., Bonin, A., Le Bras, Y., Taberlet, P. & Coissac, E. (2016) obitools: a UNIX-inspired software package for DNA metabarcoding. *Molecular Ecology Resources*, 16, 176–182.

Boyes, B.M., Linch, L.D., Pearce, D.M., Kolka, V.V. & Nash, D.J. (2021) The Kola Peninsula and Russian Lapland: a review of Late Weichselian glaciation. *Quaternary Science Reviews*, 267, 107087.

Boyes, B.M., Linch, L.D., Pearce, D.M. & Nash, D.J. (2023) The last Fennoscandian Ice Sheet glaciation on the Kola Peninsula and Russian Lapland (Part 1): ice flow configuration. *Quaternary Science Reviews*, 300, 107871.

Brauer, A., Endres, C. & Negendank, J.F.W. (1999) Lateglacial calendar year chronology based on annually laminated sediments from Lake Meerfelder Maar, Germany. *Quaternary International*, 61, 17–25.

Bronk Ramsey, C. (1995) Radiocarbon calibration and analysis of stratigraphy: the OxCal program. *Radiocarbon*, 37(2), 425–430.

Bronk Ramsey, C.A. (1994) Analysis of chronological information and radiocarbon calibration: the program OxCal. *Archaeological Computing Newsletter*, 41, 11–16.

Cai, P., Huang, Q., Zhang, X. & Chen, H. (2006) Adsorption of DNA on clay minerals and various colloidal particles from an Alfisol. *Soil Biology & Biochemistry*, 38, 471–476.

Campbell, I.D., McDonald, K., Flannigan, M.D. & Kringayark, J. (1999) Long-distance transport of pollen into the Arctic. *Nature*, 399, 29–30. Available from: https://doi.org/10.1038/19891

Capo, E., Giguet-Covex, C., Rouillard, A., Nota, K., Heintzman, P.D., Vuillemin, A. et al. (2021) Lake sedimentary DNA research on past terrestrial and aquatic biodiversity: overview and recommendations. *Quaternary*, 4, 6.

Clarke, C.L., Alsos, I.G., Edwards, M.E., Paus, A., Gielly, L., Haflidason, H. et al. (2020) A 24,000-year ancient DNA and pollen record from the Polar Urals reveals temporal dynamics of arctic and boreal plant communities. *Quaternary Science Reviews*, 247, 106564.

Clarke, C.L., Edwards, M.E., Gielly, L., Ehrich, D., Hughes, P.D.M., Morozova, L.M. et al. (2019) Persistence of arctic-alpine flora during 24,000 years of environmental change in the Polar Urals. *Scientific Reports*, 9, 19613. Available from: https://doi.org/10.1038/s41598-019-55989-9

Cohen, K.M. & Gibbard, P. (2011) Global Chronostratigraphical Correlation Table for the Last 2.7 Million Years Subcommission on Quaternary Stratigraphy (International Commission on Stratigraphy), Cambridge, England. http://quaternary.stratigraphy.org/charts/

Core Team (2017) R: a language and environment for statistical computing. - R Foundation for Statistical Computing, Vienna, Austria. URL http://www.R-project.org/. Last access January, 2024.

Cuffey, K.M. & Clow, G.D. (1997) Temperature, accumulation, and ice sheet elevation in central Greenland through the last deglacial transition. *Journal of Geophysical Research: Oceans*, 102, 26383–26396.

Cuffey, K.M., Clow, G.D., Alley, R.B., Stuiver, M., Waddington, E.D. & Saltus, R.W. (1995) Large Arctic temperature change at the Wisconsin-Holocene Glacial Transition. *Science*, 270, 455–458.

Davydova, N. & Servant-Vildary, S. (1996) Late Pleistocene and Holocene history of the lakes in the Kola Peninsula, Karelia and the North-Western part of the East European plain. *Quaternary Science Reviews*, 15, 997–1012.

Dewald, A., Heinze, S., Jolie, J., Zilges, A., Dunai, T. & Rethemeyer, J. et al. (2013) Cologne AMS, a dedicated center for accelerator mass spectrometry in Germany. *Nuclear Instruments & Methods in Physics Research Section B-Beam Interactions with Materials and Atoms*, 294, 18–23.

Elina, G.A., Arslanov, H.A., Klimanov, V.A. & Usova, L.I. (1995) Vegetation and Holocene climatochronology in the Lovozero Plain, Kola Peninsula (inferred based on spore-pollen diagrams of a hummocky bog). *Botanicheskii zhurnal*, 80(3), 1–16 [In Russian].

Elshin, Y.u. A. (Ed.) (1969) *Surface water resources of the USSR. V1. Kola peninsula*. Leningrad: Gidrometeoizdat, 134 p. [in Russian].

Elven, R., Murray, D.F., Razzhivin, V. & Yurtsev, B.A. (2011) *Checklist of the Panarctic Flora (PAF)*. Oslo: Natural History Museum, University of Oslo. Available from: http://panarcticflora.org/flora. [Accessed 26th February 2024].

Elverhøi, A., Fjeldskaar, W., Solheim, A., Nyland-Berg, M. & Russwurm, L. (1993) The Barents Sea Ice Sheet—a model of its growth and decay during the last ice maximum. *Quaternary Science Reviews*, 12, 863–873.

Gordon, A.D. & Birks, H.J.B. (1972) Numerical methods in Quaternary palaeoecology. I. Zonation of pollen diagrams. *New Phytologist*, 71, 961–979.

Gorodkov, B.N. (Ed.) (1953) *Flora of Murmansk Region. 1*. Moscow & Leningrad: Academy of Sciences of the USSR, p. 254. [In Russian].

Grave, M.K., Gunova, V.S., Devyatova, E.I., Lavrova, M.A., Lebedeva, R.M. & Samsonova, L.Ya.et al. (1969) Mikulinskoye mezhlednikoviye na yugo-vostoke Kolskogo poluostrova [Mikulinian interglacial in the southeastern Kola Peninsula]. In: Grave, M.K. & Koshechkin, B.I. (Eds.) *Main problems of geomorphology and anthropogen stratigraphy of the Kola Peninsula*. Leningrad: Nauka Press, pp. 25–56. [in Russian].

Gribova, S., Isachenko, T. & Lavrenko, E. (Eds.) (1980) *Vegetation of the European part of the USSR*. Leningrad: Science Publishers. p. 236. [In Russian].

© 2025 The Authors *Journal of Quaternary Science* Published by John Wiley & Sons Ltd. 

Grimm, E.C.A. (1987) CONISS: a FORTRAN 77 program for stratigraphically constrained cluster analysis by method of incrimination sum of squares. *Computers & Geosciences*, 13(1), 13–35.
Grimm, E.C.A. (1990) TILIA and TILIA.GRAPH: PC spreadsheet and graphics software for pollen data. *INQUA Working Group on Data Handling Methods Newsletter*, 4, 5–7.
Grimm, E.C.A. (1992) TILIA and TILIA-graph: pollen spreadsheet and graphic programs. *Volume of abstracts 8th International Palynological Congress, Aix-en-Provence*, 56.
Grimm, E.C.A. (2004) *Tilia and TG View Version 2.0.2*. Illinois: Illinois State Museum, Research and Collector Center.
Hättestrand, C., Kolka, V. & Johansen, N. (2008) Cirque infills in the Khibiny mountains, Kola Peninsula, Russia—palaeoglaciological interpretations and modern analogues in East Antarctica. *Journal of Quaternary Science*, 23, 165–174.
Head, M.J. & Gibbard, P.L. (2015) Formal subdivision of the quaternary system/period: past, present, and future. *Quaternary International*, 383, 4–35. Available from: https://doi.org/10.1016/j.quaint.2015.06.039
Heaton, T.J., Blaauw, M., Blackwell, P.G., Bronk Ramsey, C., Reimer, P.J. & Scott, E.M. (2020) The IntCal20 approach to radiocarbon calibration curve construction: a new methodology using Bayesian splines and errors-in-variables. *Radiocarbon*, 62, 821–863.
Hill, M.O. & Gauch, H.G. (1980) Detrended correspondence analysis: an improved ordination technique. *Vegetatio*, 42, 47–58.
Huang, Y.T. (2014) *Studies on carbon and DNA preservation in allophonic soils and paleosols on Holocene tephras in New Zealand*. Hamilton, New Zealand: University of Waikato.
Huang, S., Stoof-Leichsenring, K.R., Liu, S., Courtin, J., Andreev, A.A. & Pestryakova, L.A. et al. (2021) Plant sedimentary ancient DNA from Far East Russia covering the last 28 ka reveals different assembly rules in cold and warm climates. *BioAxiv*. [Preprint]. Available from: https://doi.org/10.1101/2020.12.11.406108
Hughes, A.L.C., Gyllencreutz, R., Lohne, Ø.S., Mangerud, J. & Svendsen, J.I. (2016) The last Eurasian ice sheets—a chronological database and time-slice reconstruction, DATED-1. *Boreas*, 45, 1–45.
Hyvärinen, H. (1976) Flandrian pollen deposition rates and tree-line history in northern Fennoscandia. *Boreas*, 5, 163–175.
Ilyashuk, E.A., Ilyashuk, B.P., Kolka, V.V. & Hammarlund, D. (2013) Holocene climate variability on the Kola Peninsula, Russian Subarctic, based on aquatic invertebrate records from lake sediments. *Quaternary Research*, 79, 350–361.
ICS (2013) *International Commission on Stratigraphy*. Available at: https://stratigraphy.org/ [Accessed February 2025].
Jongman, R.H.G., ter Braak, C.A.J.F. & van Tongeren, O.F.R., (Eds.) (1987) *Data analysis in community and landscape ecology*. The Nederlands: Pudoc Wageningen.
Jørgensen, T., Haile, J., Möller, P., Andreev, A., Boessenkool, S., Rasmussen, M. et al. (2012) A comparative study of ancient sedimentary DNA, pollen and macrofossils from permafrost sediments of northern Siberia reveals long-term vegetational stability. *Molecular Ecology*, 21, 1989–2003.
Kleman, J. & Glasser, N. (2007) The subglacial thermal organisation (STO) of ice sheets. *Quaternary Science Reviews*, 26, 585–597.
Kleman, J. & Hättestrand, C. (1999) Frozen-bed Fennoscandian and Laurentide ice sheets during the Last Glacial Maximum. *Nature*, 402, 63–66.
Kleman, J., Hättestrand, C., Borgström, I. & Stroeven, A. (1997) Fennoscandian palaeoglaciology reconstructed using a glacial geological inversion model. *Journal of Glaciology*, 43, 283–299.
Kolka, V.V., Korsakova, O.P., Nikolaeva, S.B. & Yevzerov, V. (2008) *The Late Pleistocene interglacial, late glacial landforms and Holocene neotectonics of the Kola Peninsula. Field Excursion. 33 IGC, The Nordic Countries*. Apatity, Kola Peninsula, Russia: Geological Institute of KSC RAS.
Konstantinova, N.A., Koryakina, A.S. & Makarova, O.A., (Eds.) (2003) Red Data Book of Murmansk Region. Murmansk: Murmansk Book Publishing House, pp.400 [In Russian].
Korsakova, O. (2020) Upper Pleistocene and Holocene stratigraphy in the Kola Peninsula and Northern Karelia (N–W Russia): marine and glacial units. *Quaternary International*, 605–606, 108–125. Available from: https://doi.org/10.1016/j.quaint.2020.11.040
Korsakova, O., Kolka, V. & Semenova, L. (2016a) Late Pleistocene stratigraphy according to the sediment sequence from eastern Kola Peninsula, Ponoi River valley (north-western Russia). *Quaternary International*, 420, 280–293. Available from: https://doi.org/10.1016/j.quaint.2015.11.101
Korsakova, O.P., Kolka, V.V., Tolstobrova, A.N., Lavrova, N.B., Tolstobrov, D.S. & Shelekhova, T.S. (2016b) Lithology and late postglacial stratigraphy of bottom sediments in isolated basins of the White Sea coast exemplified by a small lake in the Chupa settlement area (Northern Karelia). *Stratigraphy and Geological Correlation*, 24, 294–312.
Kozhin, M.N., Borovichev, E.A., Kravchenko, A.V., Popova, K.B. & Razumovskaya, A.V. (2020) Addition to the non-native flora of Murmansk Region. *Biodiversity Data Journal*, 23, 111. Available from: https://doi.org/10.14258/turczaninowia.23.4.11
Kremenetski, C., Vaschalova, T., Goriachkin, S., Cherkinsky, A. & Sulerzhitsky, L. (1997) Holocene pollen stratigraphy and bog development in the western part of the Kola Peninsula, Russia. *Boreas*, 26, 91–102.
Kremenetski, C., Vaschalova, T. & Sulerzhitsky, L. (1999) The Holocene vegetation history of the Khibiny Mountains: implications for the post-glacial expansion of spruce and alder on the Kola Peninsula, northwestern Russia. *Journal of Quaternary Science*, 14(1), 29–43.
Kremenetski, K.V., MacDonald, G.M., Gervais, B.R., Borisova, O.K. & Snyder, J.A. (2004) Holocene vegetation history and climate change on the northern Kola Peninsula, Russia: a case study from a small tundra lake. *Quaternary International*, 122, 57–68.
Krikunova, A.I., Kostromina, N.A., Savelieva, L.A., Tolstobrov, D.S., Petrov, A.Y., Long, T. et al. (2022) Late- and postglacial vegetation and climate history of the central Kola Peninsula derived from a radiocarbon-dated pollen record of Lake Kamenistoe. *Palaeogeography, Palaeoclimatology, Palaeoecology*, 603, 111191.
Kullman, L. (2002) Rapid recent range-margin rise of tree and shrub species in the Swedish Scandes. *Journal of Ecology*, 90, 68–77.
Kuzeneva, O.I. (1963) About the Flora of Murmansk region. *Botanicheskii Zhurnal*, 48(8), 1215–1216. [In Russian].
Kylander, M.E., Ampel, L., Wohlfarth, B. & Veres, D. (2011) High resolution X-ray fluorescence core scanning analysis of Les Echets (France) sedimentary sequence: new insights from chemical proxies. *Journal of Quaternary Science*, 26, 109–117.
Lenz, M., Savelieva, L., Frolova, L., Cherezova, A., Moros, M. & Baumer, M.M. et al. (2020) Lateglacial and Holocene environmental history of the central Kola region, northwestern Russia revealed by a sediment succession from Lake Imandra. *Boreas*, 50, 76–100. ISSN 0300-9483. Available from: https://doi.org/10.1111/bor.12465
Litt, T. & Stebich, M. (1999) Bio- and chronostratigraphy of the Lateglacial in the Eifel region. *Quaternary International*, 61, 5–16.
Liu, S., Stoof-Leichsenring, K.R., Kruse, S., Pestryakova, L.A. & Herzschuh, U. (2020) Holocene vegetation and plant diversity changes in the North-Eastern Siberian tree line region from pollen and sedimentary ancient DNA. *Frontiers in Ecology and Evolution*, 8, 560243. Available from: https://doi.org/10.3389/fevo.2020.560243
Lohne, Ø.S., Mangerud, J. & Birks, H.H. (2013) Precise 14C ages of the Vedde and Saksunarvatn ashes and the Younger Dryas boundaries from western Norway and their comparison with the Greenland Ice Core (GICC05) chronology. *Journal of Quaternary Science*, 28, 490–500.
Lundqvist, J. (1986) Late Weichselian glaciation and deglaciation in Scandinavia. *Quaternary Science Reviews*, 5, 269–292.
Lundqvist, J. & Saarnisto, M. (1995) Summary of project IGCP-253. *Quaternary International*, 28, 9–18.
MacDonald, G.M., Gervais, B.R., Snyder, J.A., Tarasov, G.A. & Borisova, O.K. (2000) Radiocarbon dated *Pinus sylvestris* L. wood from beyond tree-line on the Kola Peninsula, Russia. *The Holocene*, 10, 143–147.
Mangerud, J., Gyllencreutz, R., Lohne, Ø. & Svendsen, J.I. (2011) Glacial history of Norway. In: Ehlers, J., Gibbard, P. & Hughes, P., (Eds.) *Quaternary Glaciations – Extent and Chronology*. Amsterdam: Elsevier.
Manly, B.F.J. (1992) *The Design and Analysis of Research Studies*. Cambridge: Cambridge University Press.

© 2025 The Authors *Journal of Quaternary Science* Published by John Wiley & Sons Ltd. 

Merkt, J. (1994) The Alleröd—Duration and climate as derived from laminated lake sediments Terra Nostra. *Schriftenreihe der Alfred-Wegener Stiftung*, 1(94), 59–63.

Merkt, J. & Müller, H. (1999) Varve Chronology and Palynology of the Late Glacial in Northwest Germany from lacustrine sediments of Hämelsee in Lower Saxony. *Quaternary International*, 61, 41–59.

Mishkin, B.A. (1953) *Flora of the Khibiny Mts., its analysis and history*. Moscow & Leningrad: Academy of Sciences of the USSR, 113 p. [In Russian].

Mitrofanov, F.P., (Ed.) (1995) *Geology of the Kola Peninsula (Baltic Shield)*. Apatity: Kola Science Centre of Russian Academy of Sciences.

Mitrofanov, F.P. (Ed.) (2001) *Geological Map of the Kola Peninsula. Scale of 1:1,000,000*. Apatity: Press KNTs RAN. [in Russian].

Moiseenko, T.I. & Yakovlev, V.A. (1990) *Anthropogenic transformations of water ecosystems in Kola Peninsula*. Leningrad: Nauka, 221 pp. [in Russian].

Moiseenko, T.I., Morgunov, B.A., Gashkina, N.A., Megorskiy, V.V. & Pesiakova, A.A. (2018) Ecosystem and human health assessment in relation to aquatic environment pollution by heavy metals: case study of the Murmansk region, northwest of the Kola Peninsula, Russia. *Environmental Research Letters*, 13, 065005. Available from: https://doi.org/10.1088/1748-9326/aab5d2

Moiseenko, T.I., Sharov, A.N., Vandish, O.I., Kudryavtseva, L.P., Gashkina, N.A. & Rose, C. (2009) Long-term modification of Arctic lake ecosystems: reference condition, degradation under toxic impacts and recovery (case study Imandra Lakes, Russia). *Limnologica*, 39, 1–13.

Nichols, R.V., Vollmers, C., Newsom, L.A., Wang, Y., Heintzman, P.D., Leighton, M. et al. (2018) Minimizing polymerase biases in metabarcoding. *Molecular Ecology Resources*, 18, 927–939.

Niemelä, J. (1993) *Quaternary Deposits of Finland and Northwestern Part of Russian Federation and Their Resources. Scale 1: 1,000,000*. Espoo: Geological Survey of Finland.

Niemeyer, B., Epp, L.S., Stoof-Leichsenring, K.R., Pestryakova, L.A. & Herzschuh, U. (2017) A comparison of sedimentary DNA and pollen from lake sediments in recording vegetation composition at the Siberian tree line. *Molecular Ecology Resources*, 17, e46–e62.

Nikolaeva, S.B. (2001) Paleoseismic events in the northeastern Baltic Shield and their geologotectonic setting. *Geomorfologia*, 4, 66–74.

Nikolaeva, S., Lavrova, N. & Denisov, D. (2017b) A catastrophic holocene event in the lake bottom sediments of the Kola region (northeastern Fennoscandian shield). *Doklady Earth Sciences*, 473, 308–312.

Nikolaeva, S.B., Lavrova, N.B. & Denisov, D.B. (2017a) Detailed paleoseismological research on the flank of the Lake Imandra depression (Kola region): new approaches and results. *Doklady Akademii Nauk*, 473(1), 88–92.

Nikolaeva, S.B., Nikonov, A.A., Shvarev, S.V. & Rodkin, M.V. (2018) Detailed paleoseismological research on the flank of the Lake Imandra depression (Kola region): new approaches and results. *Russian Geology and Geophysics*, 59, 697–708.

Nikonov, A.A. (1966) Stratigrafiya i paleogeografiya antropogena Kolskogo poluostrova iprilegayushschikh oblastei [Quaternary stratigraphy and paleogeography of the Kola Peninsula and adjacent areas]. In: Grichuk, V.P. (Ed.) *Verhniy Pleistocen. Stratigrafya I Absolyutnaya Geohronologia [Upper Pleistocene. Stratigraphy and geochronology]*. Moscow: Nauka Press, pp. 92–105. [in Russian].

Nikonov, A.A. & Vostrukhina, T.M. (1964) K stratigrafii antropogena severo-vostochnoy chasti Kolskogo poluostrova [On the Anthropocene stratigraphy in the North-Eastern Kola Peninsula]. *Doklady Akademii Nauk USSR*, 158(4), 104–107. [in Russian].

Nogarotto, A., Noormets, R., Chauhan, T., Mollenhauer, G., Hefter, J. & Grotheer, H. et al. (2023) Coastal permafrost was massively eroded during the Bølling-Allerød warm period. *Communications Earth & Environment*, 4, 350.

Olyunina, O.S., Polyakova, E.I. & Romanenko, F.A. (2008) Diatom assemblages from Holocene sediments of the Kola Peninsula. *Doklady Earth Sciences*, 423, 1343–1347.

Orlova, M.A., Lukina, N.V., Tutubalina, O.V., Smirnov, V.E., Isaeva, L.G. & Hofgaard, A. (2013) Soil nutrient's spatial variability in forest–tundra ecotones on the Kola Peninsula, Russia. *Biogeochemistry*, 113, 283–305.

Panarctic Flora. *Annotated checklist of the Panarctic Flora (PAF) vascular plants*. (2011) Available at: http://panarcticflora.org/. [Accessed April 2023].

Pansu, J., Giguet-Covex, C., Ficetola, G.F., Gielly, L., Boyer, F., Zinger, L. et al. (2015) Reconstructing long-term human impacts on plant communities: an ecological approach based on lake sediment DNA. *Molecular Ecology*, 24, 1485–1498.

Parducci, L., Alsos, I.G., Unneberg, P., Pedersen, M.W., Han, L., Lammers, Y. et al. (2019) Shotgun environmental DNA, pollen, and macrofossil analysis of lateglacial lake sediments from southern Sweden. *Frontiers in Ecology and Evolution*, 7, 189.

Parducci, L., Bennett, K.D., Ficetola, G.F., Alsos, I.G., Suyama, Y., Wood, J.R. et al. (2017) Ancient plant DNA in lake sediments. *New Phytologist*, 214(3), 924–942.

Parducci, L., Väliranta, M., Salonen, J.S., Ronkainen, T., Matetovici, I. & Fontana, S.L. et al. (2015) Proxy comparison in ancient peat sediments: pollen, macrofossil and plant DNA. *Philosophical Transactions of the Royal Society, B: Biological Sciences*, 370, 20130382.

Patton, H., Hubbard, A., Andreassen, K., Auriac, A., Whitehouse, P.L., Stroeven, A.P. et al. (2017) Deglaciation of the Eurasian ice sheet complex. *Quaternary Science Reviews*, 169, 148–172.

Paus, A. & Haugland, V. (2017) Early- to mid-Holocene forest-line and climate dynamics in southern Scandes Mountains inferred from contrasting megafossil and pollen data. *The Holocene*, 27, 361–383.

Pedersen, M.W., Ruter, A., Schweger, C., Friebe, H., Staff, R.A., Kjeldsen, K.K. et al. (2016) Postglacial viability and colonization in North America's ice-free corridor. *Nature*, 537, 45–49. Available from: https://doi.org/10.1038/nature19085

Petrova, O.V. & Razumovskaya, A.V. (2017) Vascular plants of Imandra Lake. *Botanicheskij zhurnal*, 102(1), 62–78. [In Russian, abstract in English].

Pietramellara, G., Franchi, M., Gallori, E. & Nannipieri, P. (2001) Effect of molecular characteristics of DNA on its adsorption and binding on homoionic montmorillonite and kaolinite. *Biology and Fertility of Soils*, 33, 402–409.

Pillar, V.D. (1999) How sharp are classifications? *Ecology*, 80(8), 2508–2516.

Pillar, V.D.P. & Orlóci, L. (1996) On randomization testing in vegetation science: multifactor comparisons of relevé groups. *Journal of Vegetation Science*, 7, 585–592.

Poliakova, A., Brown, A.G. & Alsos, I.G. (2024) Exotic pollen in sediments from the high Arctic Lake Tenndammen, Svalbard archipelago: diversity, sources, and transport pathways. *Palynology*, 48(3), 2287005. Available from: https://doi.org/10.1080/01916122.2023.2287005

Poliakova, A., Håkansson, L.M., Schomacker, A. et al. (in preparation). Arctic vegetation resilient to the environmental change: 700 years of ancient plant DNA, macro-remains, microfossils and palaeohydrological changes from Western Svalbard. *Quaternary Science Reviews*.

Poyarkova, A.I. (Ed.) (1954) *Flora of Murmansk region. 2*. Moscow & Leningrad: Academy of Sciences of the USSR, 289 p. [In Russian].

Poyarkova, A.I. (Ed.) (1956) *Flora of Murmansk region. 3*. Moscow & Leningrad: Academy of Sciences of the USSR, 450. [In Russian].

Poyarkova, A.I. (Ed.) (1959) *Flora of Murmansk region. 4*. Moscow & Leningrad: Academy of Sciences of the USSR, 394 p. [In Russian].

Poyarkova, A.I. (Ed.) (1966) *Flora of Murmansk region. 5*. Moscow & Leningrad: Science Publishers, 549 p. [In Russian].

Prentice, H.C. (1982) Late Weichselian and early Flandrian vegetational history of Varanger peninsula, northeast Norway. *Boreas*, 11, 187–208.

Rare and Protected Plants and Animals of the Murmansk Region. 1990. (2nd edition, revised and supplemented). Murmansk: Murmansk Book Publishing House, p. 192.

Rasmussen, S.O., Andersen, K.K., Svensson, A.M., Steffensen, J.P., Vinther, B.M. & Clausen, H.B. et al. (2006) A new Greenland ice core chronology for the last glacial termination. *Journal of Geophysical Research: Atmospheres*, 111, D06102.

Red Data Book of Russian Federation (Plants and Fungi). (2008) In: Bardunov, L.V., & Novikov, V.S. (Eds.) Moscow, Russia: KMK Press, p. 855p. [in Russian].

© 2025 The Authors *Journal of Quaternary Science* Published by John Wiley & Sons Ltd. 

Reimer, P.J., Austin, W.E.N., Bard, E., Bayliss, A., Blackwell, P.G., Bronk Ramsey, C. et al. (2020) The IntCal20 Northern Hemisphere radiocarbon age calibration curve (0–55 cal kBP). *Radiocarbon*, 62(4), 725–757. Available from: https://doi.org/10.1017/RDC.2020.41

Reimer, P.J., Bard, E., Bayliss, A. & Warren Beck, J. (2013) Selection and treatment of data for radiocarbon calibration: an update to the international calibration (Intcal) criteria. *Radiocarbon*, 55, 1923–1945.

Rethemeyer, J., Fülop, R.H., Höfle, S., Wacker, L., Heinze, S. & Hajdas, I. et al. (2013) Status report on sample preparation facilities for C-14 analysis at the new Cologne AMS center. *Nuclear Instruments & Methods in Physics Research Section B-Beam Interactions with Materials and Atoms*, 294, 168–172.

Revéret, A., Rijal, D.P., Heintzman, P.D., Brown, A.G., Stoof-Leichsenring, K.R. & Alsos, I.G. (2023) Environmental DNA of aquatic macrophytes: the potential for reconstructing past and present vegetation and environments. *Freshwater Biology*, 68, 1929–1950.

Rijal, D.P., Heintzman, P.D., Lammers, Y., Yoccoz, N.G., Lorberau, K.E., Pitelkova, I. et al. (2021) Sedimentary ancient DNA shows terrestrial plant richness continuously increased over the Holocene in northern Fennoscandia. *Science Advances*, 2021, 7.

Rousseau, D.-D., Duzer, D., Cambon, G., Jolly, D., Poulsen, U. & Ferrier, J. et al. (2003) R., Long distance transport of pollen to Greenland. *Geographical research letters. Atmospheric Science*, 30(1), 1765. Available from: https://doi.org/10.1029/2003GL017539

Russian State Water Register. (2009) Available at: http://textualru/gvr/index.php?card=155366. [Accessed May 2023].

Seppä, H. (1996) Post-glacial dynamics of vegetation and tree-line in the far north of Fennoscandia. *Fennia*, 174(1), 1–96.

Seppä, H. & Birks, H.J.B. (2001) July mean temperature and annual precipitation trends during the Holocene in the Fennoscandian tree-line area: pollen-based climate reconstructions. *The Holocene*, 11(5), 527–539. https://doi.org/10.1191/095968301680223486

Seppä, H., Bjune, A.E., Telford, R.J., Birks, H. & Veski, S. (2009) Last nine-thousand years of temperature variability in Northern Europe. *Climate of the Past*, 5, 523–535. Available from: https://doi.org/10.5194/cp-5-523-2009

Seppä, H., MacDonald, G.M., Birks, H.J.B., Gervais, B.R. & Snyder, J.A. (2008) Late-Quaternary summer temperature changes in the northern-European tree-line region. *Quaternary Research*, 69, 404–412.

Shilova, O.S., Romanenko, F.A., Kolka, V.V. & Denisov, D.B. (2019) Holocene environmental changes in the Northern Khibiny mountains (Kola Peninsula) inferred by diatom analysis of lake sediments. *Geomorphology RAS*, 2019, 91–101. [In Russian].

Shvarev, S.V. (2003) Postglacial tectonic motions and formation of the Lake Imandra terraces (Kola Peninsula). *Geomorfologia*, 4, 97–104.

Sjögren, P., Edwards, M.E., Gielly, L., Langdon, C.T., Croudace, I.W., Merkel, M.K.F. et al. (2017) Lake sedimentary DNA accurately records 20th century introductions of exotic conifers in Scotland. *New Phytologist*, 213, 929–941. Available from: https://doi.org/10.1111/nph.14199

Snyder, J.A., Macdonald, G.M., Forman, S.L., Tarasov, G.A. & Mode, W.N. (2000) Postglacial climate and vegetation history, north-central Kola Peninsula, Russia: pollen and diatom records from Lake Yarnyshnoe-3. *Boreas*, 29, 261–271.

Soininen, E.M., Gauthier, G., Bilodeau, F., Berteaux, D., Gielly, L. & Taberlet, P. et al. (2015) Data from: highly overlapping winter diet in two sympatric lemming species revealed by DNA metabarcoding. *PLoS One*, 10, e0115335.

Solovieva, N. & Jones, V.J. (2002) A multiproxy record of Holocene environmental changes in the central Kola Peninsula, northwest Russia. *Journal of Quaternary Science*, 17, 303–318.

Solovieva, N., Tarasov, P.E. & MacDonald, G. (2005) Quantitative reconstruction of Holocene climate from the Chuna Lake pollen record, Kola Peninsula, northwest Russia. *The Holocene*, 15, 141–148.

Sorsa, P. (1965) Pollenanalytische Untersuchungen zur spatquartaren Vegetations und Klimaetwiklung im ostlichen Nordfinnland. *Annales Botanici Fennici*, 2, 301–413. [In German].

Stroeven, A.P., Hättestrand, C., Kleman, J., Heyman, J., Fabel, D., Fredin, O. et al. (2016) Deglaciation of Fennoscandia. *Quaternary Science Reviews*, 147, 91–121.

Svendsen, J.I., Alexanderson, H., Astakhov, V.I., Demidov, I., Dowdeswell, J.A., Funder, S. et al. (2004) Late Quaternary ice sheet history of northern Eurasia. *Quaternary Science Reviews*, 23, 1229–1271.

Sønstebø, J.H., Gielly, L., Brysting, A.K., Elven, R., Edwards, M., Haile, J. et al. (2010) Using next-generation sequencing for molecular reconstruction of past Arctic vegetation and climate. *Molecular Ecology Resources*, 10, 1009–1018.

Taberlet, P., Coissac, E., Pompanon, F., Gielly, L., Miquel, C., Valentini, A. et al. (2007) Power and limitations of the chloroplast trnL (UAA) intron for plant DNA barcoding. *Nucleic Acids Research*, 35, e14.

Ter Braak, C.P. & Smilauer, P. (2002) *CANOCO Reference manual and CanoDraw for Windows User's Guide: software for Canonical Community Ordination*. NY, USA: Microcomputer Power Editors, Ithaka.

Thiagarajan, N., Subhas, A.V., Southon, J.R., Eiler, J.M. & Adkins, J.F. (2014) Abrupt pre-Bølling-Allerød warming and circulation changes in the deep ocean. *Nature*, 511(7507), 75–78. Available from: https://doi.org/10.1038/nature13472

Tolstobrova, A., Tolstobrov, D., Kolka, V. & Korsakova, O. (2016) Late glacial and postglacial history of Lake Osinovoye (Kola region) inferred from sedimentary diatom assemblages. *Proceedings of the Karelian Research Centre of the Russian Academy of Sciences*, 5, 106–116. [In Russian].

Väliranta, M., Salonen, J.S., Heikkilä, M., Amon, L., Helmens, K. & Klimaschewski, A. et al. (2015) Plant macrofossil evidence for an early onset of the Holocene summer thermal maximum in northernmost Europe. *Nature Communications*, 6, 1–8. Available from: https://doi.org/10.1038/ncomms7809

Vaschalova, T.V. & Klimanov, V.A. (1987) Kolichestvennye paleoklimaticheskiye rekonstruktsii v Khibinakh kak analogi klimata buduschego (metodika, rezultaty). *Vestnik Moskovskogo Universiteta, Seriya 5 (Geografia)*, 1, 84–88. [in Russian].

Velichko, A.A., Faustova, M.A., Pisareva, V.V. & Karpukhina, N.V. (2017) History of the Scandinavian ice sheet and surrounding landscapes during Valday ice age and the Holocene. *Ice and Snow*, 57, 391–416. [in Russian].

Wang, Y., Pedersen, M.W., Alsos, I.G., De Sanctis, B., Racimo, F., Prohaska, A. et al. (2021) Late Quaternary dynamics of Arctic biota from ancient environmental genomics. *Nature*, 600, 86–92. Available from: https://doi.org/10.1038/s41586-021-04016-x

Wastegård, S. (2022) The Holocene of Sweden—a review. *GFF*, 144(2), 126–149. Available from: https://doi.org/10.1080/11035897.2022.2086290

Whittaker, R.J. (1993) Plant population patterns in a glacier foreland succession: pioneer herbs and later-colonizing shrubs. *Ecography*, 16, 117–136.

Willerslev, E., Davison, J., Moora, M., Zobel, M., Coissac, E., Edwards, M.E. et al. (2014) Fifty thousand years of Arctic vegetation and megafaunal diet. *Nature*, 506(7486), 47–51.

Williams, J.W., Spanbauer, T.L., Heintzman, P.D., Blois, J., Capo, E., Goring, S.J. et al. (2023) Strengthening global-change science by integrating aeDNA with paleoecoinformatics. *Trends in Ecology & Evolution*, 38, 946–960.

Yevzerov, V.Y. & Nikolaeva, S.B. (2008) Terminal stages of the evolution of sheet and mountain glaciations in Khibiny. *Doklady Earth Sciences*, 421, 792–795. [In Russian].

Zastrozhnov, A.S., Minina, E.A., Shkatova, V.K. & Tarnogradsky, V.D. (2014) *Karta chetvertichnykh obrazovanyi territorii Rossiyskoi Federatsii. Masshtab 1:2500000 (A map of Quaternary deposits of the Russian Federation territory. Scale 1:2500000)*. St. Petersburg: All-Russian Geological Institute (VSEGEI) Press. [in Russian]. Available from: http://www.vsegei.com/ru/info/quaternary-2500/

Zhamoida, A.I., Girshgorn, L.C.H., Kovalevsky, O.P., Oleynikov, A.N., Prozorovskaya, E.L. & Khramov, A.N. et al. (2006) *Stratigraphichesky Kodeks Rossii, Isdanie Tretie (Stratigraphic Code of Russia (third ed.)*. St. Petersburg: All-Russian Geological Institute (VSEGEI) Press. [in Russian].

Zimmermann, H., Raschke, E., Epp, L., Stoof-Leichsenring, K.R., Schirrmeister, L. & Schwamborn, G. et al. (2017b) The history of tree and shrub taxa on Bol'shoy Lyakhovsky Island (New Siberian Archipelago) since the last interglacial uncovered by sedimentary

© 2025 The Authors *Journal of Quaternary Science* Published by John Wiley & Sons Ltd. 

ancient DNA and pollen data. *Genes*, 8(10), 273. Available from: https://doi.org/10.3390/genes8100273

Zimmermann, H.H., Raschke, E., Epp, L.S., Stoof-Leichsenring, K.R., Schwamborn, G. & Schirrmeister, L. et al. (2017a) Sedimentary ancient DNA and pollen reveal the composition of plant organic matter in Late Quaternary permafrost sediments of the Buor Khaya Peninsula (north-eastern Siberia). *Biogeosciences*, 14, 575–596.

Zykov, D.S. (2001) Recent Geodynamics of the North Karelian Zone (Baltic Shield) GEOS, Moscow. *Transactions of GIN RAS*, 534, 146. [in Russian].

© 2025 The Authors *Journal of Quaternary Science* Published by John Wiley & Sons Ltd. 